A PARAMAGNETIC RESONANCE SPECTROMETER FOR THE INVESTIGATION OF FREE RADICAL SPECIES IN SOLIDS AT LOW TEMPERATURES

A THESIS

presented by

CLAUDE B. TAYLOR, B.Sc.

to the University of St. Andrews
in application for the Degree of
Master of Science, March, 1961.

DECLARATION

I hereby declare that this thesis has been composed by me, is a record of work carried out by me, and that it has not been previously presented for a higher degree.

Claude B. Taylor

CERTIFICATE

I certify that Claude Brechin Taylor, B.Sc., has spent four terms as a research student in the Physical Laboratory of the United College of St. Salvator and St. Leonard in the University of St. Andrews, that he has fulfilled the conditions of Ordinance No. 51 of the University Court of St. Andrews and that he is qualified to submit the accompanying thesis in application for the Degree of Master of Science.

(Supervisor)

CAREER

I matriculated in October, 1953 in the United College of St. Salvator and St. Leonard in the University of St. Andrews and followed a course leading to graduation in June, 1957 with the Degree of Bachelor of Science with Honours in Natural Philosophy. In October 1957 I was admitted by the Senatus Academicus of the same University as a research student in the Department of Natural Philosophy in the same College and have since then been engaged upon the work described in this thesis.

INDEX

CHAPTER 4. (Continued) Page

CHAPTER 1

Introductory

The use of paramagnetic resonance as a tool for the detection, identification and structural investigation of free radicals has become widespread during the last few years. Identification and structural investigation are frequently complicated by the effect on the absorption lines of interactions between neighbouring free radicals. Two types of interaction are commonly encountered in solids and in concentrated solutions. One is the interaction between the magnetic dipole moments of neighbouring radicals, which results in a broadening of the absorption line and removal of the nuclear hyperfine structure. The other is due to the quantum mechanical exchange interaction between the spins of neighbouring radicals resulting in the effect known as exchange narrowing, whereby the absorption lines are narrowed in the centre and broadened in the wings, the shape tending to change from Gaussian to Lorentzian.

To reduce these interactions in order to obtain a clearer indication of the structure of the radical itself, unaffected by its neighbours, the distance between neighbouring molecules must be increased. There are three ways of doing this. In the first the free radicals can be dissolved in a suitable diamagnetic solution until a dilution is

reached at which the fully resolved hyperfine pattern of the radical is obtained. This method suffers from two defects however. As the solution is diluted the number of free radicals in a given volume of solution decreases. Since the volume of solution that can be inserted in a microwave resonant cavity can only be a small fraction of the total volume of the cavity if severe electrical damping is not to result, it is clear that the limit of sensitivity of the spectrometer may be reached before the solution has been diluted sufficiently to produce the resolved hyperfine pattern. Further, and more important, in solution any anisotropic hyperfine splitting, produced by the interaction between the dipole moments of the free electrons and the dipole moments of the nuclei to which they are bonded, is averaged to zero by the rapid tumbling motion of the radicals and the consequent random orientation of the radical bonds about the direction of the applied magnetic field. The hyperfine effects are discussed in greater detail in Chapter 2.

The second possibility would be to create a mixed crystal where the radicals would be present in small concentrations in a diamagnetic matrix. Each radical would then occupy a fixed position in the crystal structure and would be well separated from its nearest paramagnetic neighbours. Free radical concentrations of 1 per 10^3 to 10^8 diamagnetic molecules would be suitable, the exact concentration depending on the type and sensitivity of the spectro-

meter employed, and on the type of spectrum expected, i.e. number of lines and their relative intensity. The chemical difficulties of preparing such crystals would be great, however. Many free radicals cannot be isolated in stable form and the choice of a suitable diamagnetic matrix would depend on previous knowledge of the size and structure of the particular radical to be investigated.

The third possibility is to create the free radicals in situ by bombarding with ionising radiation crystals of parent molecules which might be likely to produce free radicals of the type required. When an organic crystal is bombarded by radiation, whose quantum of energy is of the order of, or greater than, the energy of any of the covalent bonds within the crystal, there are several possible processes which may take place. Electrons in the organic molecule may be excited to energy states above the ground state or acquire enough energy to enable them to be liberated from their parent molecules, leaving behind positive ions, which may be free radicals. Electrons liberated from their parent molecules may cause disruption of bonds in neighbouring molecules resulting in the formation of new uncharged molecules, free atoms, free radicals and vacant lattice sites where other molecular fragments may become trapped.

Much evidence exists to show that free radicals can be created in this way. Some evidence, such as the coloration of organic

substances, (e.g. L1, 2, 3, 4, 5), changes in the photoconductivity of organic crystals, (e.g. K1), and in the conductivity of commonly used insulators,(e.g. F1, 2, 3, 4, 5, 6, 7, 8, M1), upon exposure to radiation of different types, may be indications of the presence of free radicals, but the most conclusive evidence of free radical creation by ionising radiation has been produced by paramagnetic resonance.

The lifetime of any free radical moving about in a crystal at room temperature in the presence of the fragments of other molecular disruptions is extremely short. Recombination may occur in several ways, neutral molecules with saturated covalent bonds again being formed. The dynamic concentrations of radicals produced by U.V. and X-irradiation are too small to be detected even by paramagnetic resonance. Techniques have been developed which enable the free radicals to be trapped before they can recombine. In the most commonly used of these the substance to be irradiated is dissolved in a hydrocarbon solution, which is known to freeze to a transparent rigid glass. The solution is then frozen to liquid nitrogen temperature and irradiated with U.V. light, when it is found that a concentration of free radicals is built up, which may be examined by paramagnetic resonance, and which remains as long as the mixture is kept in the frozen state, disappearing quickly when the temperature is raised. It is believed that the excess energy released

during the splitting of a molecule warms the surrounding glass sufficiently to permit the free radicals to move apart, the glass freezing again to trap the radicals before they can recombine. The solvent used to form the glass must be chosen carefully since, at the correct temperature, it must be sufficiently rigid to prevent recombination of the radicals, yet not so rigid as to prevent them moving apart as the glass warms slightly. Three mixtures of this type in common use are E.P.A. (5 parts ether, 5 parts iso-pentane and 2 parts ethanol, by volume), P.He.H. (3 parts iso-pentane and 2 parts cyclohexane), and I.M_4P (4 parts methylcyclohexane and 1 part isopentane). Bijl and Rose Innes, (Bl, Rl), have experimented with solid solutions at room temperature. The specimens to be investigated were dissolved with Perspex in chloroform. Evaporation of the chloroform from the solution on a glass plate left a thin film, which was irradiated at room temperature for periods up to half an hour. The films became coloured and paramagnetic resonance was found in certain cases, notably with p-phenylenediamine and Wurster's base.

In all experiments with the trapping techniques mentioned the interaction effects of neighbouring molecules are negligible but the orientation of the radicals with respect to the applied magnetic field is random so that the anisotropic hyperfine pattern is not resolved, the anisotropic interaction producing only a line broadening.

TABLE 1.1

Bond	Energy (e.v.)	Source	Wavelength A°
C - H	4.32	Methane	2,870
N - H	3.895	Ammonia	3,180
O - H	4.75	Water	2,660
C - C	3.65	Paraffins	3,400
C = C	6.56	Olefins and Cyclic Compounds	1,890
C ≡ C	8.61	Acetylene Hydrocarbons	1,440
C - O	3.47	Aliphatic Primary Alcohols	3,570
C = O	7.20	Formaldehyde	1,720
C - N	2.95	Amines	4,210
C = N	5.75	Estimated value	2,160
C ≡ N	8.75	Hydrogen Cyanide	1,420
C - S	2.92	Mercapatans and thio-ethers	4,250
C = S	5.60	Estimated value	2,220

If free radicals could be created in organic crystals so that they occupied vacant lattice sites in which they would remain surrounded by diamagnetic neighbours and with their positions and orientations maintained in the crystalline lattice by the crystalline fields, then fully resolved hyperfine patterns should be obtained yielding exact knowledge of the structure and interactions of the radical itself without hindrance by neighbouring radicals and the effects produced by random orientation.

U.V. irradiation is the most selective means of producing free radicals by breakage of bonds. Table 1.1 shows the energies of a number of organic bonds deduced by Pauling (P1) together with the wavelength of the equivalent quantum of radiation. The use of a series of ultra-violet filters enables a control to be exercised on the bonds to be broken. Thus C - H bond breakages would not be expected if light of wavelength less than 3,000A^{o} were filtered out, whereas we might still expect C - N bond breakage. The radiation damage induced by U.V. light at room temperature is impermanent because of the short lifetime of the radical species created. X- and γ-ray irradiation yields permanent damage of several sorts, and Atherton and Whiffen have reported the recording of an electron resonance spectrum from a single crystal of glycollic acid, irradiated at room temperature with a 200 Curie ^{60}Co γ-ray source, which they attribute to the radicals carboxy-hydroxy-methyl, $\dot{H}OCHCOOH$ trapped

in the crystal in specific orientations, (W1, see also W2). We believed that it might be possible to produce such orientated radicals in crystalline samples using U.V. light, if we first lowered the temperature to reduce the thermal motion of the radicals enabling them to be more easily trapped in vacant lattice sites. This thesis is an account of the design of a spectrometer to investigate this problem. Several experiments have been conducted on irradiated crystals at temperatures in the range 4.2°K to 1.2°K, and at liquid air temperature but up to the present no resulting radicals have been detected. Chapter 2 contains a brief resumé of some of the theory of paramagnetic resonance which applies to our problem, and of the interpretation of free radical spectra.

In Chapter 3 the construction and operation of the spectrometer is described in detail.

Chapter 4 is a report on the experimental programme undertaken to date, and on the sensitivity of the spectrometer. Some suggestions which might lead to successful experiments are included.

CHAPTER 2

Paramagnetic Resonance and Its Application To Free Radical Studies

The theory of the paramagnetism of free radicals and the information obtainable from the study of their paramagnetic resonance spectra is summarised in detail, with references, in the recent text-book by Professor Ingram. (I1). Other reviews of general para-magnetic resonance theory include (B2, 3, 4, 5). What follows is only a very brief summary of some of the more important free radical processes which our spectrometer was designed to investigate. We mention first some aspects of paramagnetic resonance theory necessary for the work described in Chapters 3 and 4, and then consider what information can be gleaned from the type of spectra which the spectrometer is capable of investigating.

(2.a.) Paramagnetism of Free Radicals

Certain atoms, ions and molecules are known to possess permanent magnetic moments due to the presence of magnetic dipoles. They are called paramagnetic. The magnetic dipoles are a consequence of the atom, ion or molecule possessing a partly filled electron shell. Most stable molecules and ions possess even numbers of electrons. The electrons which take part in the bonding between atoms in organic molecules form bonds, largely covalent in character, by the sharing

of one or more pairs of electrons. A free radical may be defined as "a molecule or part of a molecule in which the normal chemical binding has been modified so that an unpaired electron is left associated with the system". Certain molecules do, however, exist which possess unpaired electrons as part of their normal chemical binding e.g. O_2, NO.

The paramagnetism of free radicals arises from the magnetic moment associated with this unpaired electron. At room temperature and below the separation between the lowest orbital level ($L = 0$) of this electron and the next highest ($L = \pm 1$) is very much greater than kT, where k is Boltzmann's constant and T is the absolute temperature, so that we may expect in free radicals that the population of states with L other than zero will be virtually nil. (The effect of a small amount of spin-orbit coupling will be discussed later).

In any system of free spins the orientation of magnetic moments will be random in zero magnetic field. If a D.C. magnetic field is applied the magnetic moments can line up in only two directions, parallel and anti-parallel to the direction of the applied field, corresponding to magnetic spin quantum numbers of $\pm \frac{1}{2}$. The electrons can thus exist in one of two energy levels whose energy difference is $g\beta H$, where g is the spectroscopic splitting factor, β is the Bohr magneton and H the applied field.

The Maxwell-Boltzmann expression for the population ratio of the number of electrons, N_1, in the upper lying state, to the number, N_2, in the lower lying state is given by:-

$$\frac{N_1}{N_2} = e^{-\frac{g\beta H}{kT}} \qquad \ldots\ldots\ldots (2.1)$$

If there are N_0 molecules per gm. then the net extra population of the lowest level per gm. is given by:-

$$\Delta N = N_2 - N_1 = N_0\left[\frac{1 - e^{-\frac{g\beta H}{kT}}}{1 + e^{-\frac{g\beta H}{kT}}}\right] \qquad \ldots\ldots\ldots (2.2)$$

(2.b.) <u>The Resonance Condition</u>

If now an alternating R.F. magnetic field is applied to the system of spins, perpendicular to H, transitions will be induced between these two electronic levels when the quantum of energy of the alternating field is equal to the difference in energy between the levels.

$$h\nu = g\beta H \qquad \ldots\ldots\ldots (2.3)$$

where h is Planck's constant and ν is the frequency of the alternating magnetic field.

From (2.3) we see that paramagnetic resonance absorption will take place at any value of magnetic field H, and the corresponding frequency. H and ν are usually chosen so that the best compromise between sensitivity and cost and convenience of operation is obtained.

(2.c.) Paramagnetic Resonance at Microwave Frequencies

The number of transitions induced between the two energy levels will be proportional to the population difference in (2.2). We see from this equation that the population difference is increased by increase of H and by decrease of T. The decrease of T is affected only by the availability of liquefied gases but from (2.3) we see that increase of H must be considered together with the consequent increase in ν. The magnetic field H must be very uniform over the volume of the paramagnetic sample if line broadening due to magnet inhomogeneities is not to result. About 0.1 gauss over the volume of the sample is adequate for most free radical investigations. It is difficult to produce fields above 10,000 gauss to satisfy this requirement. The frequencies corresponding to fields of the order 1,000 to 10,000 gauss lie within the microwave range and it happens that the upper limits of H correspond roughly to the frequencies at which the power outputs of continuously operated klystrons are of the order of magnitude required for maximum absorption of power by the paramagnetic sample, without saturation of the resonance lines. In a microwave paramagnetic resonance spectrometer the sample is placed in a region of concentrated radio frequency alternating magnetic field in a resonant cavity placed between the poles of a magnet. The Q's obtainable using accurately designed cavities are very much higher than those obtainable at

lower frequencies with radio-frequency coils and as we shall see in Chapter 3, the Q-factor of the cavity should be large for greater sensitivity. A disadvantage of an 8mm. spectrometer, ($H \doteqdot$ 13,000 gauss), is that in the resonant cavity the regions of maximum R.F. magnetic field and minimum R.F. electric field are so small that the introduction of a specimen or specimen holder of size comparable to that in common use in 3cm. spectrometers will seriously damp the cavity, so this spectrometer, where H is as high as it can be for good homogeneity, is only more sensitive than a 3cm. spectrometer when very small samples are used. For most free radical investigations a 3cm. spectrometer, $H \doteqdot 3{,}500$ gauss is employed.

(2.d.) Variation of Temperature

We consider now the effect of lowering the temperature on the population difference between the levels, (2.2). In Table 2.1. below we have derived the ratio of population differences at certain standard low temperatures to that at room temperature. At temperatures of 20°K and above the approximation

$$e^{-\frac{g\beta H}{kT}} = e^{-\frac{h\nu}{kT}} = 1 - \frac{h\nu}{kT} \qquad \ldots\ldots\ldots (2.4)$$

holds to a good degree of accuracy but for temperatures below this point we must use the full expression (2.2). The frequency ν is taken to be 9,375 Mc/s.

TABLE 2.1

$T^{\circ}K$	290	83	20	4.2	1
Ratio of ΔN to ΔN at $290^{\circ}K$	1	3.4	13.7	56	166

Thus if we assume that all conditions in the spectrometer remain the same as the temperature is lowered, the ratios of the spectrometer sensitivities at the low temperatures to that at room temperature are given by the above figures. However, there are other factors on which the sensitivity depends which are temperature-dependent and these must be taken into account. These will be discussed in Chapters 3 and 4.

It is worthwhile noting here that much of the theory of paramagnetic susceptibilities both in static and alternating magnetic fields is derived using the approximation (2.4). At temperatures below $20^{\circ}K$, however, this approximation no longer holds, and at $1.2^{\circ}K$, the lowest limit obtained by us using liquid helium, $h\nu \doteqdot \frac{1}{2}kT$. Equations for the static mass susceptibility and for power absorptions in a microwave cavity (I1) must be rederived without approximation of the exponential if an accurate picture of the magnetic behaviour of a paramagnetic specimen at liquid helium temperatures is to be obtained.

(2.e.) Hyperfine Structure of the Resonance Lines

If the unpaired electron in the D.C. magnetic field encom-

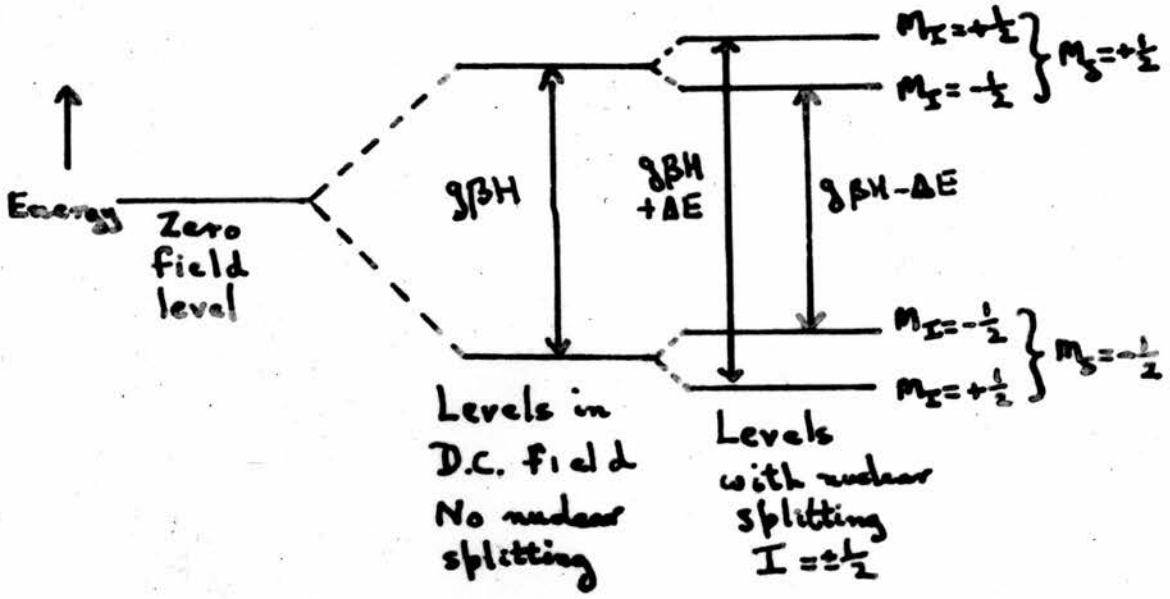

Fig. 2.1. Splitting of energy levels due to applied D.C. field, showing hyperfine splitting due to nucleus of spin $\frac{1}{2}$ and two allowed transitions.

passes in its orbital a nucleus of spin other than zero, then this nucleus will take up one of (2I + 1) possible orientations with repect to the magnetic field, where I is the nuclear spin quantum number. The nuclear magnetic moments will produce additional fields at the free electrons and each level of the electronic doublet will be split into (2I + 1) components, whose populations may for our purposes be taken to be equal. The energy levels are raised or lowered about the original value according as the magnetic field of the nucleus raises or lowers the field at the electrons. The effect on the energy levels of a nucleus of spin $\frac{1}{2}$ is shown in Fig. 2.1. Transitions between the levels are now governed by the selection rule $\Delta M_I = 0$, that is the magnetic quantum number of the nuclear spin remains unchanged during an electronic transition. In the case shown in Fig. 2.1. only two transitions can take place and since the population differences may be taken as equal for each transition, the absorption lines will be of equal intensity.

Of particular interest to the study of aromatic free radicals is the case where the orbit of the unpaired electron encompasses equally several hydrogen protons. Ingram (I1) describes in detail the effect for 2 and 3 equivalent protons. For the general case of n equivalent protons, each with spin quantum number $\frac{1}{2}$, a pattern of (n + 1) equally spaced lines will be observed with intensity distribution:-

$$1 : n : \frac{n(n-1)}{2} : \ldots\ldots : \frac{n!}{k!(n-k)!} : \ldots\ldots : n : 1 \quad \ldots\ldots\ldots \quad (2.5)$$

where k = 1, 2, ..., n - 1.

When a spectrum arises from the presence of more than one free radical, the overlapping spectra can often be separated, particularly if phase-sensitive detection of the spectrum is employed. In phase-sensitive detection the derivative of the spectrum is recorded, and the resolution of the lines is always more obvious than when video detection is employed. In many cases the hyperfine structure is either smeared out and the line broadened, or narrowed by interaction, respectively, of the magnetic moments of the free electrons with other magnetic moments, and by quantum-mechanical exchange effects.

(2.f.) Information Obtainable from the Analysis of Free Radical Spectra

We consider the information that can be obtained from a free radical in general, rather than from the type of radical we have tried to produce, since the spectrometer is capable of use in the investigation of solid free radicals in general. The information obtainable relates mainly to the following aspects of the free radical specimens:-

(i) The number of free radicals present.

(ii) Knowledge of the orbital path of the unpaired electrons; this may lead to the identification

of the radical species from several known possibilities, by the use of quantum chemical theories of the electron orbits.

(iii) The interactions between the radicals and neighbouring molecules and radicals.

(iv) The magnitude of the coupling between the almost free spin and the orbital momentum of the electrons.

(v) The derivation of an approximate Spin-Hamiltonian for the spin system.

We consider these aspects individually and briefly.

(i) The number of free radicals in a specimen can be computed by comparing the integrated line intensity with that of a known standard sample whose spectrum is recorded either simultaneously or under identically reproduced experimental conditions.

(ii) Information on the orbital of the unpaired electron may be derived from a fully resolved hyperfine pattern, since the nuclear spins which affect the energy levels of the electron can be deduced from the number of hyperfine lines, and the magnitude of the interaction with each nucleus from the spacing of the lines and their relative intensities. This can lead to identification of the radicals when their identity has not been fully established, e.g. when the radicals have been created by irradiation damage.

The hyperfine splitting in resonance absorption lines arises from two causes. The first is an anisotropic effect arising, as already explained, from the interaction of electronic and nuclear dipole moments. This anisotropic splitting shows a $(3\cos^2\theta - 1)$ variation in paramagnetic single crystals, where θ is the angle between the electron-nucleus vector and the applied magnetic field. In amorphous solids the effect averaged over all orientations produces a smeared out hyperfine structure, while in liquids the rapid tumbling motion of the molecules causes the anisotropic hyperfine splitting to be averaged to zero. The second cause of hyperfine splitting arises from the term in the spin Hamiltonian called the Fermi Contact term. To explain the isotropic splitting effect the free electron, normally considered to occupy a pure π -orbital, is assumed to have some measure of σ -orbital as well, allowing the wave-function to have a finite probability at the nuclei which the orbital encompasses. This hyperfine splitting is observed in liquids as well as solids, where the effects of interaction with neighbouring free radicals are negligible.

(iii) The effects of spin-spin interaction and exchange interaction between neighbouring free radicals, already mentioned in Chapter 1, are frequently present together in varying degrees in certain free radical specimens. In magnetically concentrated solids and in very concentrated solutions the exchange narrowing effect

will predominate (V1, P2, A1, K2, D1). In the case of the free radical diphenylpicrylhydrazyl (DPPH) calculation shows that spin-spin interaction between neighbouring radicals should produce broadening of about 30 gauss. However, the measured line width is only 2.7 gauss, due to the predominance of exchange narrowing. If DPPH is dissolved in benzene the initial effect is the broadening of the line due to the ascendancy of the spin-spin interaction over the exchange interaction. Further dilution removes the spin-spin interaction and a resolved isotropic hyperfine pattern of five lines is obtained (H1) which can be explained on the basis of equal coupling of the unpaired electron to the two nitrogen atoms in the centre of the molecule.

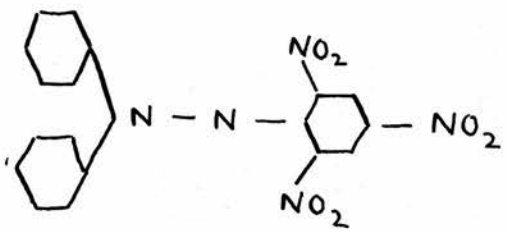

This is an elegant demonstration of the spin-spin and exchange interaction effects.

Another effect which may occur in free radical investigations is due to spin-lattice relaxation. This is the process by which electrons excited to the higher of the two energy levels return to the ground state without the emission of electromagnetic radiation. The temperature of the spin-system is raised by transitions from

lower to upper level, and thermal equilibrium with the surrounding lattice is restored by conversion of the excess magnetic energy to thermal energy via the spin-orbit coupling. Since the spin-orbit coupling in free radicals is very small, long relaxation times may be expected and saturation of the resonance lines, when the relaxation processes are not fast enough to prevent population equalisation of the two energy levels, may easily be produced.

(iv) Measurement of the magnetic field at the centre of each individual resonance pattern together with measurement of the frequency of the alternating magnetic field gives the g-value, using equation (2.3). The g-values of nearly all free radicals lie very close to the free-electron value. Departure of the g-value from the free-electron value is an indication of a certain amount of orbital momentum coupled to the spin momentum of the unpaired electron.

(v) The general Hamiltonian for any system of free radicals will consist of the following terms (B4):-

1. The energy of the Coulomb interactions between the unpaired electron and the nuclei and other electrons within the radical.
2. The potential energy of any crystalline field at the unpaired electron.
3. The energy due to a small amount of spin-orbit coupling.
4. The interaction energy of the unpaired electron with the external magnetic field.

5. The interaction energy of the magnetic moment of the unpaired electron and the magnetic moments of the nuclei encompassed by its orbital.
6. Energy due to the interactions of the nuclear magnetic moments with the external magnetic field.
7. Energy of the electrostatic interaction between the unpaired electron and the nucleons within the radical, giving rise to nuclear quadrupole moments.
8. Energy due to interactions with neighbouring molecules, the spin-spin and exchange effects.

Such a Hamiltonian is difficult to set up with any accuracy but in many cases certain of the terms can be neglected e.g. in the case of zero nuclear spin and no interaction between molecules. The general procedure in the setting up of a Spin Hamiltonian is to first try to deduce from a knowledge of the geometry of the radical, should this be known, an approximate Hamiltonian and then to find out if this empirical Hamiltonian fits the resonance absorption spectrum. If not, new terms are introduced in the empirical Hamiltonian until a rough agreement is reached.

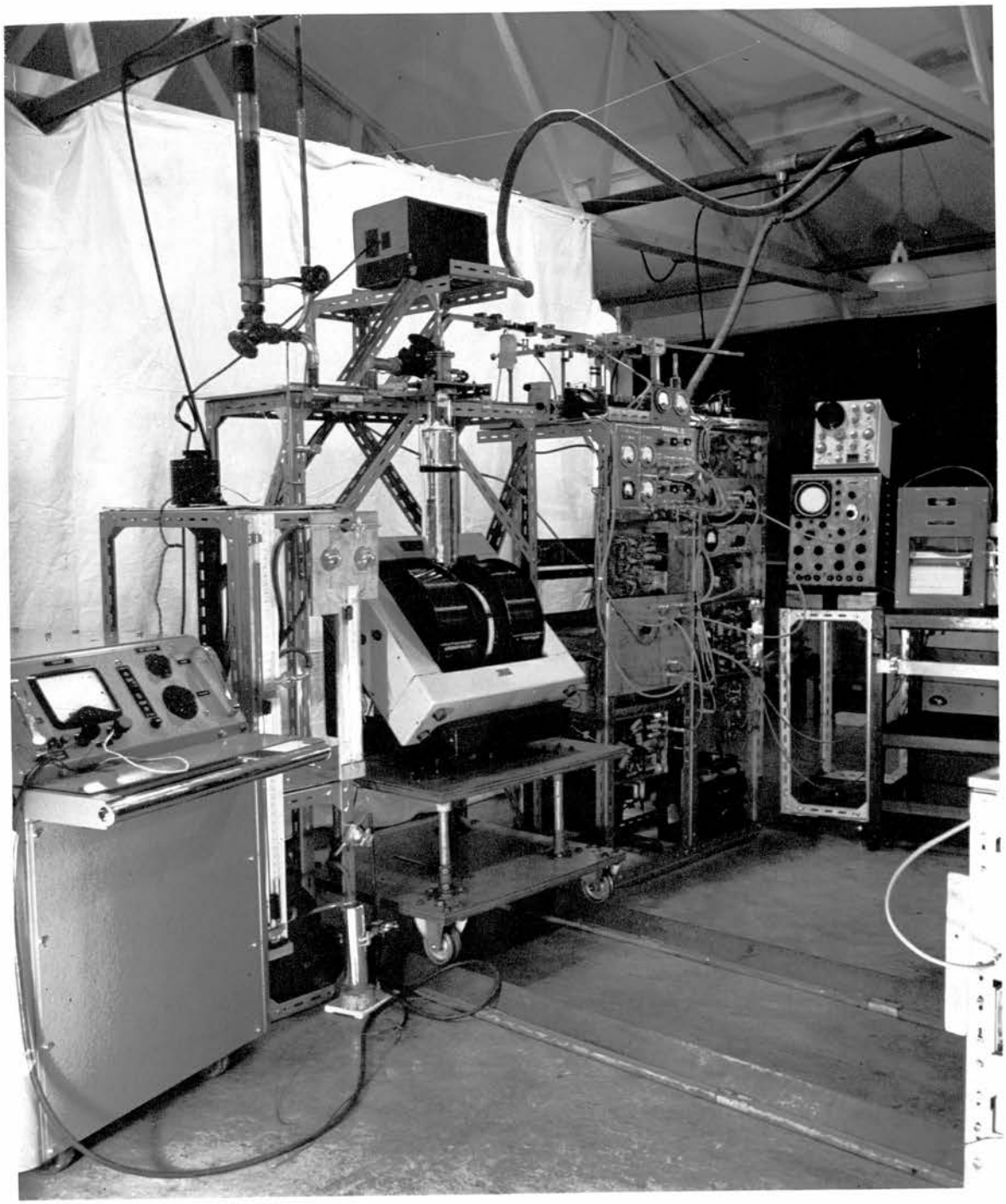

Fig. 3.1. General View of the Apparatus.

CHAPTER 3

The Apparatus

(3.a.) Design Considerations for Optimum Sensitivity

We have already seen that the best type of spectrometer for our purpose was one operating in the 3 cm. microwave range, both from the point of view of maximum difference in population between the electronic energy levels consistent with homogeneity of the D.C. magnetic field and increase of ν, and of the Q-factor of the resonant cavity. The components of the spectrometer and, in particular, the method of signal detection were required to be chosen to provide good sensitivity. The factors influencing the sensitivity in a 3 cm. spectrometer have been discussed in a paper by Feher. (F9). Consideration of the U.V. illumination problem and the limitations of space within the cryostat led to the decision to use a reflection resonant cavity. With this type of cavity some means of separating the incident and reflected microwave signals is desirable and the sensitivity is enhanced if the signal is detected as a small power change over a zero mean level, rather than a small power change over a large mean level. The usual method of achieving this is to use a balanced magic-tee bridge which, under the correct conditions of match, effectively decouples the output detector arm from the input signal arm. The analysis by Feher (F9) shows that the best sensitivity is gained by using superheterodyne detection, where

the signal to be detected is mixed at a second magic-tee with another microwave signal to produce an I.F. component, of frequency some tens of megacycles, in the side arms of the second tee, which contain detecting crystals. At low frequencies the noise generated in semiconductor crystal detectors is the main limitation on the sensitivities of spectrometers employing straight detection, but at frequencies of the order of tens of megacycles crystal noise is negligible. Since the mean power level at such a detecting crystal is of the order of the local oscillator power, for small signal voltages, the voltage produced at the detecting crystal is proportional to the microwave voltage incident upon it. Feher's analysis for a reflection cavity and a bridge magic-tee arrangement shows that the maximum voltage change transmitted to the detector arm due to a resonance absorption occurs when the two arms of the tee are correctly matched. If a reflectionless load is placed in one of these arms and the cavity in the other, the correct operating condition is that the cavity should be close to critical coupling at its resonant frequency, i.e., the VSWR in the cavity arm ~ 1. One should not work too close to the critical condition, as an absorption signal might change the coupling condition distorting the resonance line due to the sign reversal of the signal at match. At frequencies within the bandwidth of the cavity resonance the signal in the detector arm will be a function of both χ' and χ'', the dispersive and absorptive components respectively of the R.F.

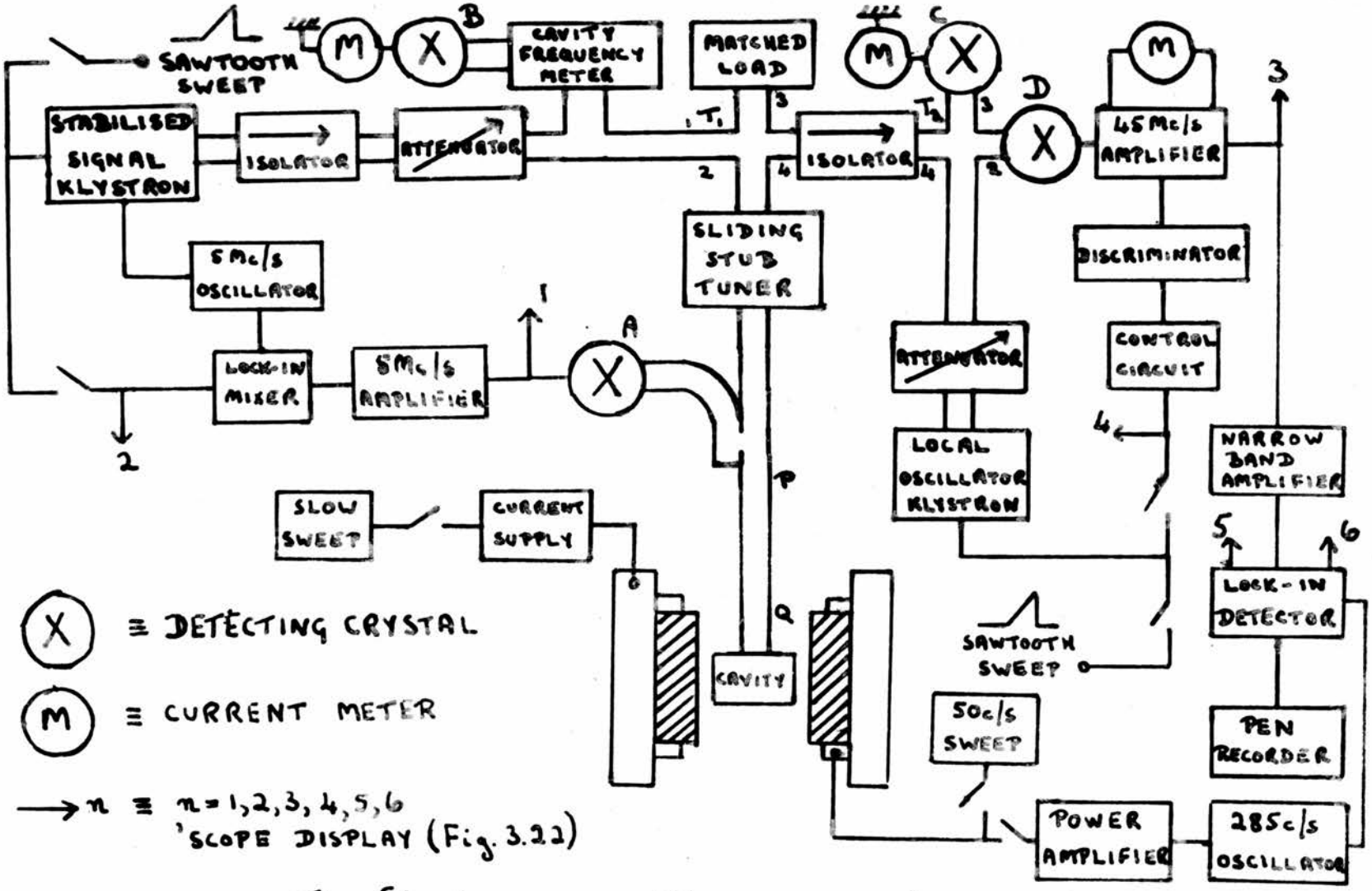

Fig. 3.2. The Spectrometer : Microwave and Electronic Components

magnetic susceptibility of the paramagnetic specimen in the cavity. The position of a sliding stub tuner, placed in the cavity arm may be adjusted to obtain at will a signal proportional to either χ' or χ''. However if the frequency of the signal klystron is locked automatically by some stabilisation scheme to the resonant frequency of the cavity, the signal will be proportional only to the power absorption associated with the imaginary susceptibility component χ'', which is the correct condition for faithful representation of a paramagnetic resonance absorption spectrum. The matching conditions may be altered in this case by variation of position and depth of the tuner until a maximum detected signal is obtained. Factors involving the sensitivity after detection of the signal at the I.F. frequency are discussed later in this chapter and in Chapter 4.

The microwave components of the spectrometer all employ the standard 3 cm. American waveguide of rectangular inner dimensions 0.900 in. x 0.400 in., this being the size in most common use at present.

(3.b.) <u>The Microwave Bridge and Electronics</u>.

A photograph of the complete apparatus is shown in Fig. 3.1. and a block diagram of microwave, electronic and magnetic components in Fig. 3.2.

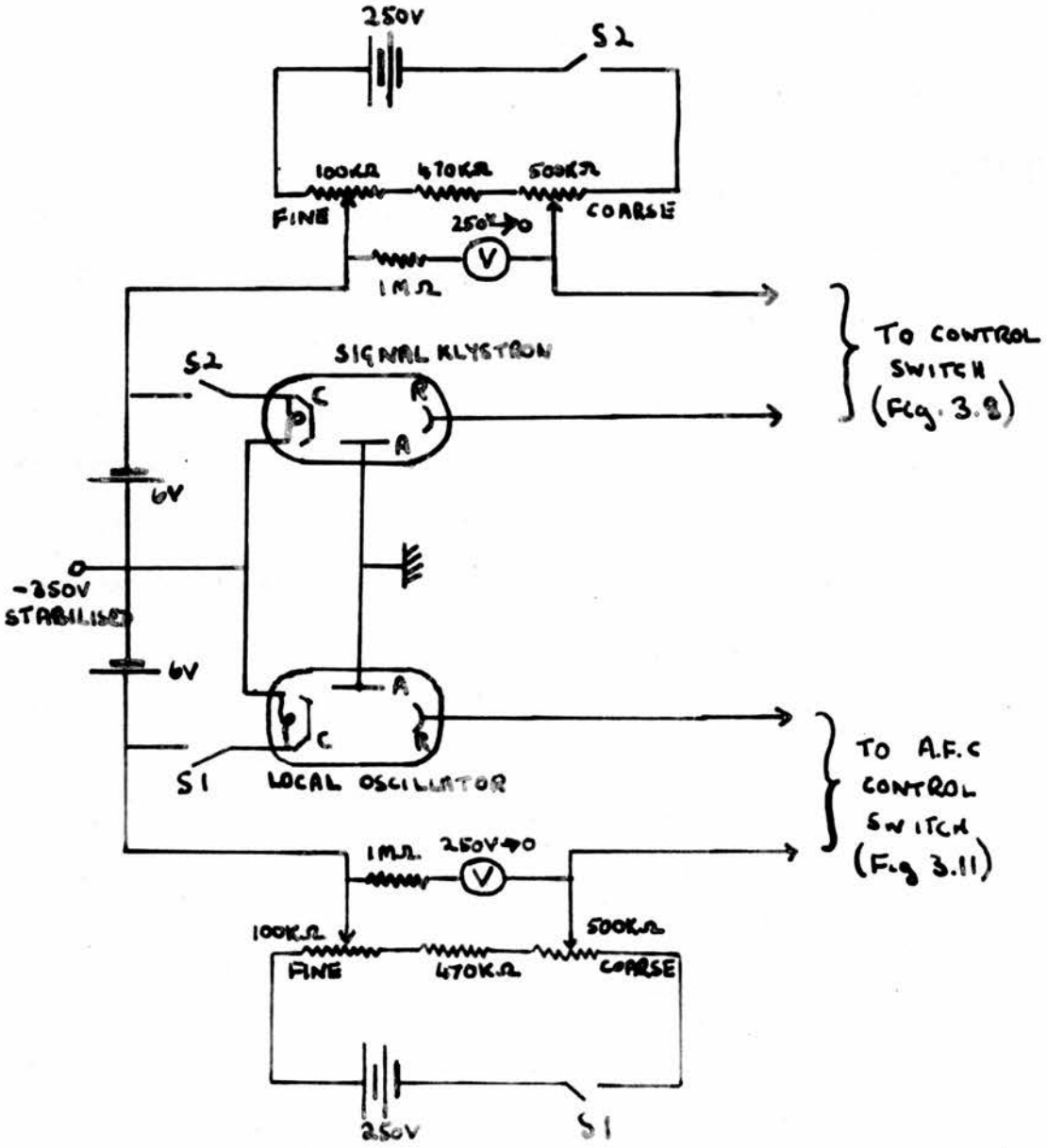

Fig. 3.3. Klystron battery supply circuits

(i) The Microwave Components.

Klystrons.

Both klystrons are of type English Electric K302, whose simple mechanical tuning with a micrometer head enables a frequency range of 9320 to 9500 Mc/s to be covered. (λ_o = 3.22 to 3.16 cm.). The battery supply circuits for the klystrons are shown in Fig. 3.3. Anode - cathode voltage for both valves is obtained from a stabilised 0 to - 350V supply, (Fig. 3.12). Reflector - cathode voltages, approximately 140V for normal operation, are obtained from separate banks of dry cells and are provided with fine and coarse control. The heater currents are taken from a 12V lead accumulator of 40 amp. hr. capacity used as two 6V cells in series. Heating by D.C. removes most 50 c/s modulation of the microwave output. Each klystron gives a maximum output of 30 mW. 20V reflector voltage change gives 30 Mc/s electronic tuning.

The initial testing and alignment of the spectrometer was carried out using 723 A/B klystrons, which operate in much the same voltage and frequency ranges and give roughly the same performance as the K302 valves.

Cavity Frequency Meter

This is of the transmission cavity type. Its cylindrical cavity operates in the H_{112} mode and is coupled to the main wave-guide line by an iris in the centre of the end wall of the cavity. The tuning is controlled by a micrometer head, a piston on the end

changing the effective length of the cavity. The tuning range is 8,800 to 10,000 Mc/s, which covers the frequency range of the klystrons. With the detector crystal B and current indicator the wavemeter is used for the following purposes:-

(a) Indication of the magnitude of signal power.

(b) Measurement of signal frequency. The accuracy claimed is 1 in 10^4.

(c) Effectiveness of signal klystron stabilisation. With no stabilisation frequency changes of the klystron are shown by intermittent jumps of the indicator needle. With stabilisation the needle remains steady.

(d) Approximate measurement of the width of the signal klystron mode in terms of frequency. (See Fig. 3.22(a))

Isolators

The reverse attenuation of the ferrite isolators used is approximately 22 db at the design frequency of 9375 Mc/s (λ_0 = 3.2 cm.) and the forward attenuation is less than 1 db. The isolator in the signal klystron arm prevents pulling of this klystron by reflected power and that in the arm between the tees prevents local oscillator power being coupled into the cavity arm.

Attenuators

The attenuators have a range of 30 db. Variation of attenuation is obtained by moving the attenuator vane across the waveguide, the level being changed by an external screw set against a mm. scale.

Magic Tees

1. This tee serves the purpose of directing and separating the incident and reflected powers to and from the resonant cavity. In conditions close to match of this tee the incident power from arm 1, the E-arm, divides equally between the loaded arm 3 and the arm 2 which leads to the cavity. It is important that a negligible part of the power passing from the input arm should be transmitted to the output arm, for an extra constant mean power level at the signal frequency would then mix with the local oscillator signal, producing at crystal D a larger I.F. signal over which any absorption signal must assert itself, the sensitivity being reduced as a result.

A Philip's Hybrid Tee manufactured from a single metal block is used. Decoupling between the input and output arms under correct conditions of operation is claimed to be better than 40 db.

2. At this tee any mismatch signal from tee 1 is mixed with the local oscillator signal. The tee was manufactured in the laboratory workshops from standard brass waveguide using dimensions suggested in (P3, M2). Adjustment of this tee is obtained by means

of tuning screws inserted in the E- and H-arms. The screws are placed sufficiently far from the junction so that no asymmetry is introduced by their presence. The admittance diagrams, (Smith charts), for two capacitive screw tuners placed $\frac{3}{8}\lambda_g$ apart, show that they can tune out all possible reflections for which the VSWR is less than 2, at the frequency for which their separation is adjusted. (R2).

A similar tee was used in place of tee 1 in the early stages of development. The manner in which the tees were adjusted for correct match is discussed later.

Sliding Stub Tuner

Changes in the load presented to tee 1 by the cavity arm, and hence in the amplitude and phase of the reflected signal, under different conditions of temperature, dielectric (liquid helium) and different positions of the cavity tuning mechanisms, may be compensated to a certain extent by the use of this variable capacitive probe whose position and depth can be controlled to close limits. Amplitude variation is effected by a micrometer head operating against a spring-loaded plunger which protrudes into the waveguide. This is mounted on a carriage which can be moved along the waveguide to provide phase variation and whose position may be closely adjusted against a vernier scale. When a free radical absorption signal is being observed, with the signal klystron frequency locked to the

cavity resonance and using a wide 50 c/s magnetic field sweep and oscilloscope presentation (Fig. 3.22(f)), judicious use of this tuner can generally be made to increase the signal to two or three times its original size. The effect is to change the coupling in the cavity arm till it has its optimum value (F9). The change in sign of the resonance signal on passing from an over-coupled to an undercoupled cavity may also be observed. However, since by far the worst source of noise in the spectrometer is microphonics arising in the cavity and cavity arm, the signal-to-noise ratio in the output is not much enhanced by this tuning process and the overall sensitivity remains much the same.

For signals too small for video detection, which require the extra sensitivity of phase-sensitive detection, the best procedure is to vary the tuner until the cavity dip on the oscilloscope display of the I.F. response curve has reached its maximum height, (Fig. 3.22(e)). Optimum coupling should then be obtained.

It should be noted that this tuner cannot compensate for the change in coupling introduced by the filling of the inner cryostat with liquid helium, using a cavity which has been adjusted for optimum coupling at room temperature. This problem will be discussed later in this chapter.

Directional Coupler

This 10 db. coupler serves to couple off part of the reflected

signal from the cavity to the beginning of the signal klystron stabilisation loop. No power is coupled from the incident signal.

Matched Load

The load in arm 3 of tee 1 consists of a wooden "clothes peg" fitted into a length of waveguide of about 15 in., (H2). The position of the peg inside the guide is varied until a reflectionless termination is obtained.

Crystal Mounts

Variable tuned crystal mounts were made in the laboratory workshops to a design used in the Clarendon Laboratory at Oxford and very similar to one described in (T1). The crystal cartridge holder was designed to take B.T.H. Type CS3-B crystals. Tuning is accomplished by alternately varying the positions of a shorting plunger in the end of the guide and two tuning screws, $\frac{3}{8}\lambda_g$ apart, on the other side of the crystal. Maximum rectified current corresponds to minimum reflected signal.

Crystals

The crystals used throughout the apparatus are silicon-tungston cartridge diodes of type B.T.H. CS3-B. At the local oscillator powers used, 1 to 10 mW, the output current of these detectors is proportional to the incident microwave voltage, so that detecting crystal D is of the type required for our conditions of match outlined in (3.a.).

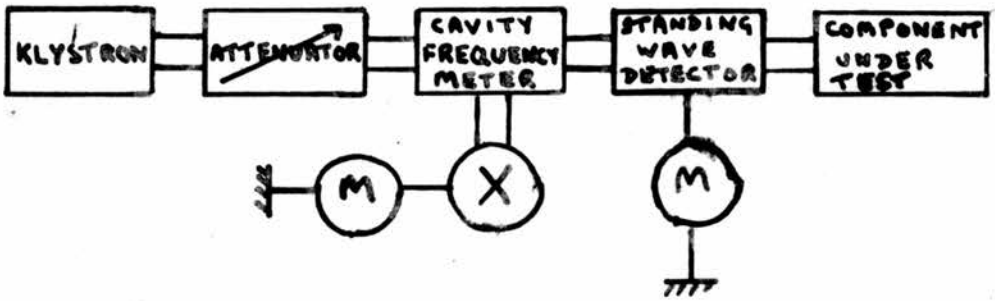

Component		V.S.W.R.
Reflectionless Load		1·025
"	"	1·035
"	"	1·05
Crystal Mount		1·05
"	"	1·05
Tee 1	E-arm	1·145
	H-arm	1·02
Tee 2	E-arm	1·15
	H-arm	1·025

Fig 3.4. Microwave Test Bench and Results of Tuning Laboratory-made Components

(ii) Alignment of Magic Tees, Crystal Mounts and Reflectionless Loads.

A microwave test bench was set up as shown schematically in Fig. 3.4 for the alignment of components built in the laboratory workshop. A 723 A/B klystron was used and the frequency set close to 9375 Mc/s. The reflectionless loads were first adjusted for minimum voltage standing wave ratio and the correct positions of the wooden pegs set with wax. Each crystal mount was then tuned for minimum standing wave ratio, the positions of the spaced tuning screws again being set with wax. Any subsequent variation of match with different crystals can be taken up by variation of the position of the shorting plunger, though this has never been found to be necessary.

Two of the reflectionless loads were then mounted on the side arms of a magic tee and the E- and H- arms tuned for minimum standing wave ratio, the positions of the tuning screws again being fixed with wax.

The results obtained for some of the components are shown beneath Fig. 3.4.

(iii) The Cavity Arm

The section PQ (Fig. 3.2.) leads from the main waveguide assembly down into the cryostat and had, therefore, to be designed to meet the various cryostatic requirements. These may be listed as follows:-

1. The cryostat should be easily detachable from the main waveguide assembly for transport to and from the helium filling station.
2. So far as is possible vibrations should not be transmitted from the cryostat to the waveguide assembly and vice versa. This serves to reduce microphonics and possible danger to the fragile glass Dewar vessels.
3. A vacuum tight seal must be provided in the waveguide somewhere near the top of the cryostat so that the cryostat may be evacuated.
4. Heat leak out of the cryostat should be kept to a minimum.

The first and third of these conditions are satisfied by the inclusion at P of a length of flexible waveguide coupled to the cryostat assembly by means of a quick release clamp. This 6 in. length of "Flexaguide" consists of a specially treated corrugated strip of beryllium copper waveguide with brass flanges, moulded in a pliable, synthetic rubber jacket. The VSWR of this assembly is 1.02 at 9,400 Mc/s and the attenuation is better than 0.075 db. The quick release clamp enables the break in the waveguide assembly to be made immediately.

The third condition is satisfied by the inclusion of a thin

mica window between two plane-faced couplers close to the point where the waveguide bends into the top of the cryostat.

The chief source of heat leak into the cryostat will be the length of waveguide, about 80 cm., passing from the cryostat top plate down through the inner Dewar vessel to the resonant cavity. A rough calculation, based on a mean thermal conductivity of brass over the temperature range $4^{\circ}K$ to $300^{\circ}K$, shows that when the helium level, at $4.2^{\circ}K$, lies 50 cm. below the top of the cryostat, at room temperature, the heat intake using standard 3 cm. American brass waveguide is equivalent to the evaporation per hour of about 4 litres of liquid helium. This is far too great a heat leak for our purposes with an inner Dewar of capacity 1 litre, even allowing for the approximations made. A waveguide of lower thermal conductivity and lower cross-sectional area would reduce this loss. The Royal Radar Establishment at Malvern has kindly supplied us with some lengths of thin-walled German-silver waveguide of the correct inner dimensions with wall thickness 0.012 in. The dimensions and rectangular shape of this waveguide do not approach the accuracy of the standard brass type but an exactly parallel heat leak calculation shows that only 200 cc. of liquid helium are lost per hour with this guide. The ratio of weights of thin-walled guide to standard brass guide is 1:12. In practice the heat leak was found to be considerably less than this, and a fill of 2/3 to 3/4 litres can be made to last up to twelve hours.

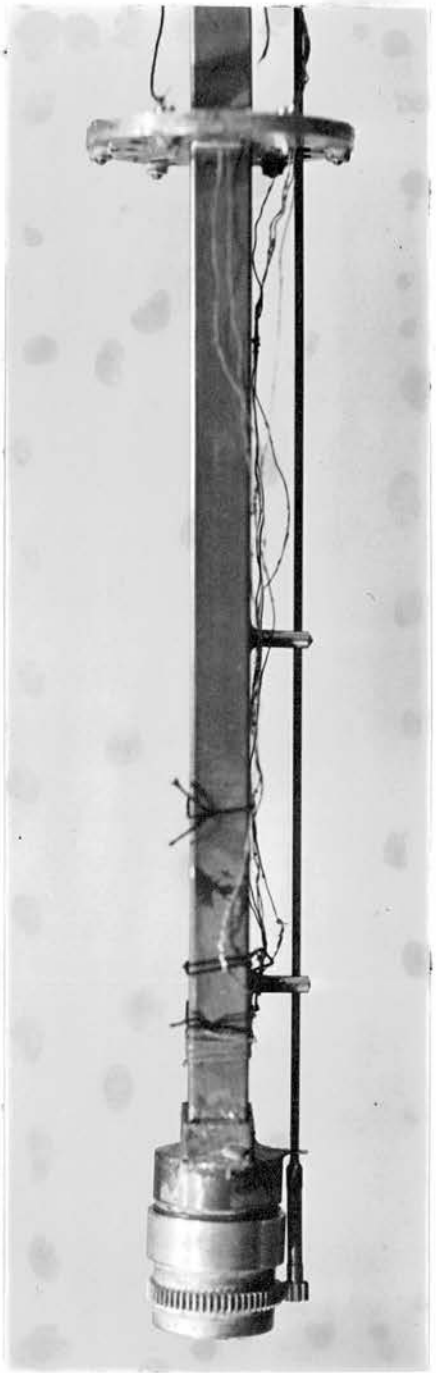

(a)

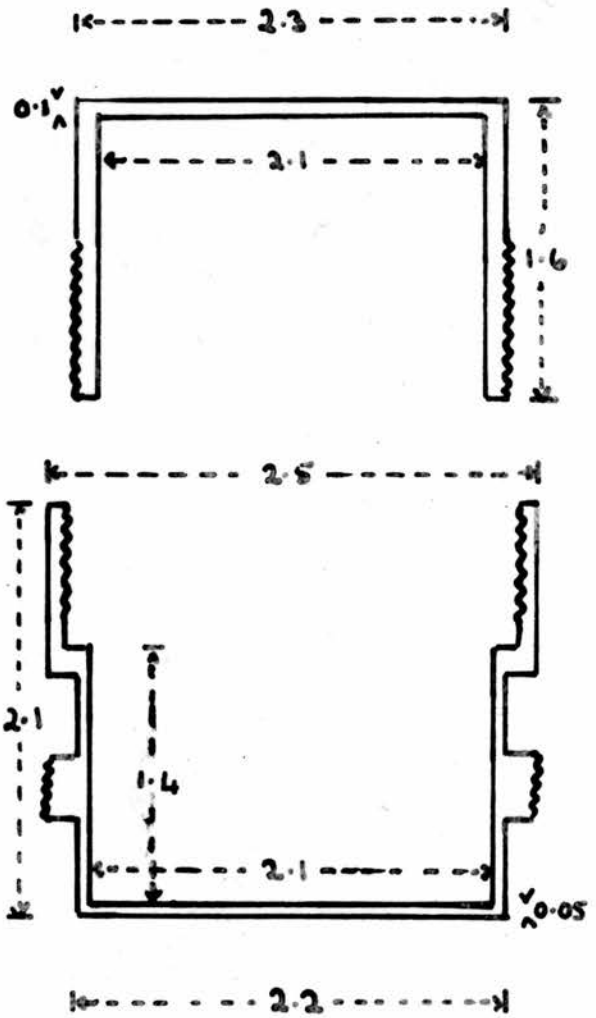

(b)

Fig. 3.5. (a) Photograph of cavity.
(b) Section of cavity. Dimensions in cms.

The German-silver waveguide was broken 18 cm. from the top of the cavity just above the tail of the inner helium Dewar and fitted into two circular brass disks of diameter $1\frac{1}{2}$ in., which serve as plain couplers held together by six 8BA screws round the circumference. (Fig. 3.5(a)). Six $\frac{1}{4}$ in. diameter holes were bored in the outer area of these couplers to facilitate the flow of helium into the Dewar. This break was made so that a change of cavity could be effected if necessary without unsoldering the original cavity from the foot of the waveguide. Any new cavity can be attached to an appropriate length of thin-walled waveguide with a similar circular coupler. In fact only one cavity has been used to date, but we shall see in Chapter 4 that one of a different sort might prove better for the future.

(iv) The Cavity

A photograph and diagram of the cavity are shown in Fig. 3.5. The choice of cavity was governed by the following requirements:-

(1) Its dimensions are limited by the available gap between the magnet pole-pieces, by the diameters of the Dewars and by the gap required between the cavity and the inner Dewar wall for the penetration of liquid helium to the foot of the Dewar.

(2) It is easier to fix the operational frequency of the spectrometer and to vary the cavity length to correspond to this frequency, than to tune the spectrometer to a fixed cavity length. The spectrometer should operate very close to the design frequency of the components,

9375 Mc/s.

(3) The specimen must be placed in the region of maximum R.F. magnetic field: it is thus simplest to use a cavity whose resonant mode is such that this region is at the foot of the cavity.

(4) Provision should be made for fine tuning of the cavity.

(5) It should be possible to illuminate the specimen with U.V. light while it sits in the cavity at low temperature.

We shall postpone discussion of (5) until we have described the cryostat in detail.

The cavity chosen was cylindrical, (Fig. 3.5.) operating in the H_{11} mode, the dominant mode. For an H_{111} cavity we have one closed loop of R.F. magnetic field and the regions of maximum magnetic field occur in the centre of top and bottom faces.

The resonant wavelength for a circular cavity in this mode is given by the equation (M2)

$$\lambda_o = \frac{2}{\sqrt{\left(\frac{2x_{11}}{\pi D}\right)^2 + \frac{1}{L^2}}} \qquad \ldots\ldots (3.1)$$

where λ_o = free space wavelength of the resonant frequency.

D = internal diameter of the cavity.

L = internal length of the cavity.

x_{11} = first root of $J'_1(x) = 0$.

Equation (3.1) may be written:-

$$(fD)^2 = \left(\frac{c\chi_{11}}{\pi}\right)^2 + \left(\frac{c}{2}\right)^2\left(\frac{D}{L}\right)^2 \quad \ldots\ldots (3.2)$$

where c is the velocity of light and f the resonant frequency.

The diameter D of the cavity was limited by virtue of the requirement (1) to 2.1 cm.

Substituting this value of D in (3.2) and using the values λ_o = 3.2 cm., f = 9,375 Mc/s we obtain L = 3.56 cm.

Consideration of the cut-off wavelength formulae for modes in circular waveguides shows that for λ_o = 3.2 cm. and D = 2.1 cm

$$\lambda_{\text{cut-off}}\ (\text{dominant mode}) > \lambda_o > \lambda_{\text{cut-off}}\ (\text{any other mode})$$

so that for our choice of diameter and frequency no mode other than the dominant can be excited.

The length of the cavity is made variable by constructing it in two halves. These were turned from solid brass and silver-plated to reduce the wall losses. The bottom half can be screwed over the top, giving a variation in cavity length of about 4 mm., the maximum and minimum inner lengths being 3.65 and 3.25 cm. respectively, corresponding to resonant frequencies of 9320 and 9550 Mc/s in vacuo. The

resonant length for 9375 Mc/s is near the bottom of the travel of the screw, since the cavity suffered a resonant length reduction when the cavity arm is immersed in liquid helium. This change is equivalent to $2\frac{1}{2}$ rotations of the bottom of the cavity, or, since the thread of the screw is 35 turns per in., about 5% of the resonant wavelength in vacuo, or air. Before fitting on the Dewars prior to a helium run the cavity is set to the resonant length at 9375 Mc/s in air, and then screwed up a further $2\frac{1}{2}$ turns, so that it will be roughly the correct length for resonance at the same frequency when immersed in liquid helium. The change in resonant length is mainly due to the dielectric constant of the liquid helium and partly also to the change in cavity dimensions.

The cavity length may be changed, when the Dewars are in position, by a simple gearing arrangement. The internal diameter of a clock wheel, of external diameter 25 mm. and thickness 3.2 mm., was increased by turning on a lathe until it slipped over the bottom half of the cavity, to which it was soft-soldered. This wheel was geared to a smaller wheel of external diameter 4.4 mm. and the same thickness, soft-soldered on the end of a long vertical hard-drawn copper rod of diameter $^1/_{16}$ in. This rod is held parallel to the cryostat waveguide by passing it through a series of horizontal pins, (Fig. 3.5(a)). It passes through a vacuum seal at the top of the cryostat where it can be turned by a knurled knob, held by a screw to the top of the rod. (Fig. 3.15).

The tooth ratio of turning wheel to cavity wheel is 1:6. A "stainless steel" rod was originally used for this purpose but it quickly became magnetised and microphonics in the reflected signal from the cavity were very troublesome.

The screw thread must be reasonably loose to prevent the gearing mechanism from jamming. However, it should not be too loose, since the pressure of the turning mechanism may make the bottom half of the cavity take up a slight angle with respect to the top half. The effect of this is to change the matching conditions of the cavity to tee 1, and can also lead to the appearance of a second cavity resonance close in frequency to the first.

In practice the resonant length of the cavity in vacuo at room temperature is a little less than that predicted for any frequency with a purely cylindrical cavity.

The coupling of the cavity to the end of the waveguide is important as mentioned earlier in this Chapter. Iris coupling through a circular hole in the end-plate of the waveguide and a hole of equal diameter in the top of the cavity is used. The end-plate of the waveguide is in the form of a rectangular sleeve with walls of height 6 mm. which fits over the end of the thin-walled guide. To fix the cavity to the foot of the guide the end-plate was first soft-soldered to the top of the cavity, then pushed over the end of the guide and soft-soldered to the outside faces. The diameter of the coupling iris

was increased until the optimum value is reached. This value may be determined by video display of the cavity response (Fig. 3.22(a)) and from the signals obtained from a known sample of DPPH (Fig. 3.22 (f)). The condition of match is that no power should be reflected from the cavity at its resonant frequency. The cavity dip should thus fall as the iris diameter is enlarged, (undercoupled cavity), reach a minimum, (critically coupled cavity), and then rise again, (overcoupled cavity). Further, the DPPH resonance absorptions should show maximum size at the correct condition of coupling.

It has already been remarked that variation of coupling round about the critical condition may be obtained using the sliding stub-tuner in the cavity arm, but that it cannot compensate for the change of coupling which occurs when the cavity is filled with liquid helium. This change of coupling is due mainly to the change in cavity Q accompanying the reduced wall losses at low temperature. It has been found that a cavity critically coupled at room temperature becomes strongly overcoupled in liquid helium. Before each helium run, therefore, a polished copper plate of thickness $^{1}/_{16}$in. and rectangular dimensions just slightly less than the inner dimensions of the waveguide was slipped into the section of thin-walled waveguide beneath the join, and pushed down over the coupling iris. This plate had a smaller coupling iris at its centre of the right diameter to produce critical coupling in liquid helium. In this way the same cavity

could be used for work at both room and liquid helium temperatures.

Tuning of the cavity to the frequency of the incident microwave power may be accomplished by use of the gearing arrangement already described. In the earlier stages of development a finer tuning was obtained using a quartz rod passing down the centre of the waveguide, which served also as a U.V. light pipe. This arrangement is discussed later.

(v) Frequency Stabilisation of the Signal Klystron

For accurate recording of electron resonance spectra it is essential that the frequency of the incident microwave radiation should remain equal to the resonant frequency of the cavity in which the paramagnetic sample is situated, over a period greater than the time taken to record the broadest spectra, (about 10 mins.). As we have seen earlier in the chapter a signal proportional to χ'' only will be reflected from the cavity if these two frequencies are equal. At other frequencies within the bandwidth of the cavity resonance the reflected signal will contain admixtures of components proportional to χ' and χ'', and the spectrum will be distorted, while at other frequencies outside the resonant response of the cavity mismatch of the cavity arm is so bad that no signal at all is detected and the energy stored within the cavity becomes negligible, both factors resulting in loss of the signal. We require, therefore, a stabilisation scheme which holds the klystron to the resonant

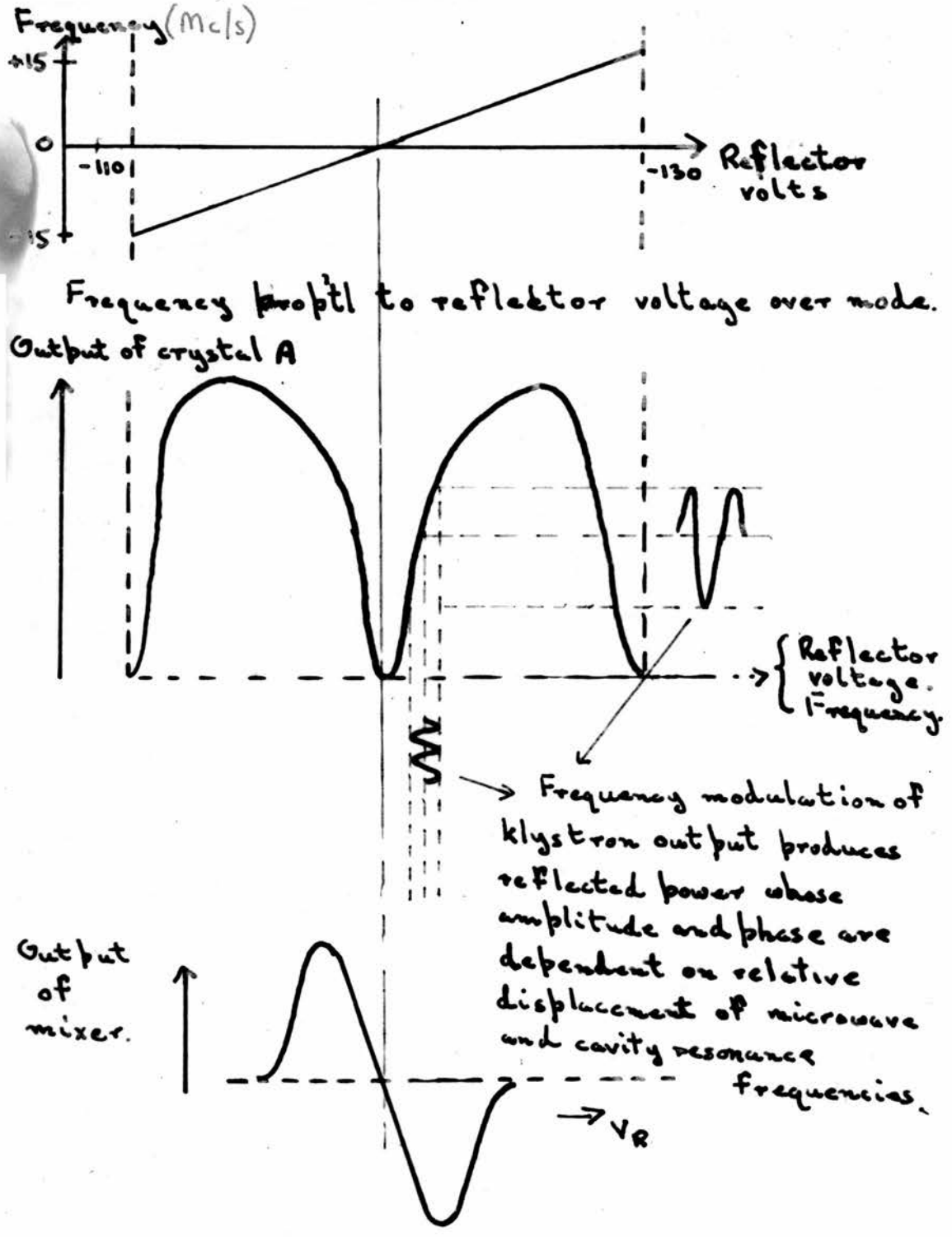

Fig. 3.6. Signal Klystron Stabilisation.

frequency of the cavity to within less than one tenth of the bandwidth of the cavity resonance. To do this we used the reflected signal of the klystron in such a way that a difference between the two frequencies is immediately corrected by the application of a correction voltage to the reflector of the klystron. A small 5 Mc/s sinusoidal sweep, of peak-to-peak amplitude 50 to 100 mV, is applied through a condenser to the reflector of the signal klystron. This amplitude modulation on the reflector produces a frequency modulation of the klystron output power (Fig. 3.6). Reflected power from the cavity will thus contain a 5 Mc/s component whose amplitude and phase are dependent on the relative displacement between the signal frequency and the cavity resonance frequency, the reflected signal being of minimum amplitude when these two frequencies are equal. Part of the reflected signal is then taken off by the 10 db directional coupler and detected at crystal A, whose output voltage will contain a 5 Mc/s component. After amplification by a tuned voltage amplifier (Fig. 3.7) the signal is fed to the grid of a pentode mixer, (Fig. 3.8), whose reference signal is derived from the same crystal oscillator, (Fig. 3.9), which modulates the klystron. The anode of this mixer is at the same potential as the klystron reflector. The phase of the incoming signal can be adjusted by judicious tuning of the tank-circuits of the tuned amplifier, so that the sign of the correction voltage applied to the reflector at the anode of the mixer

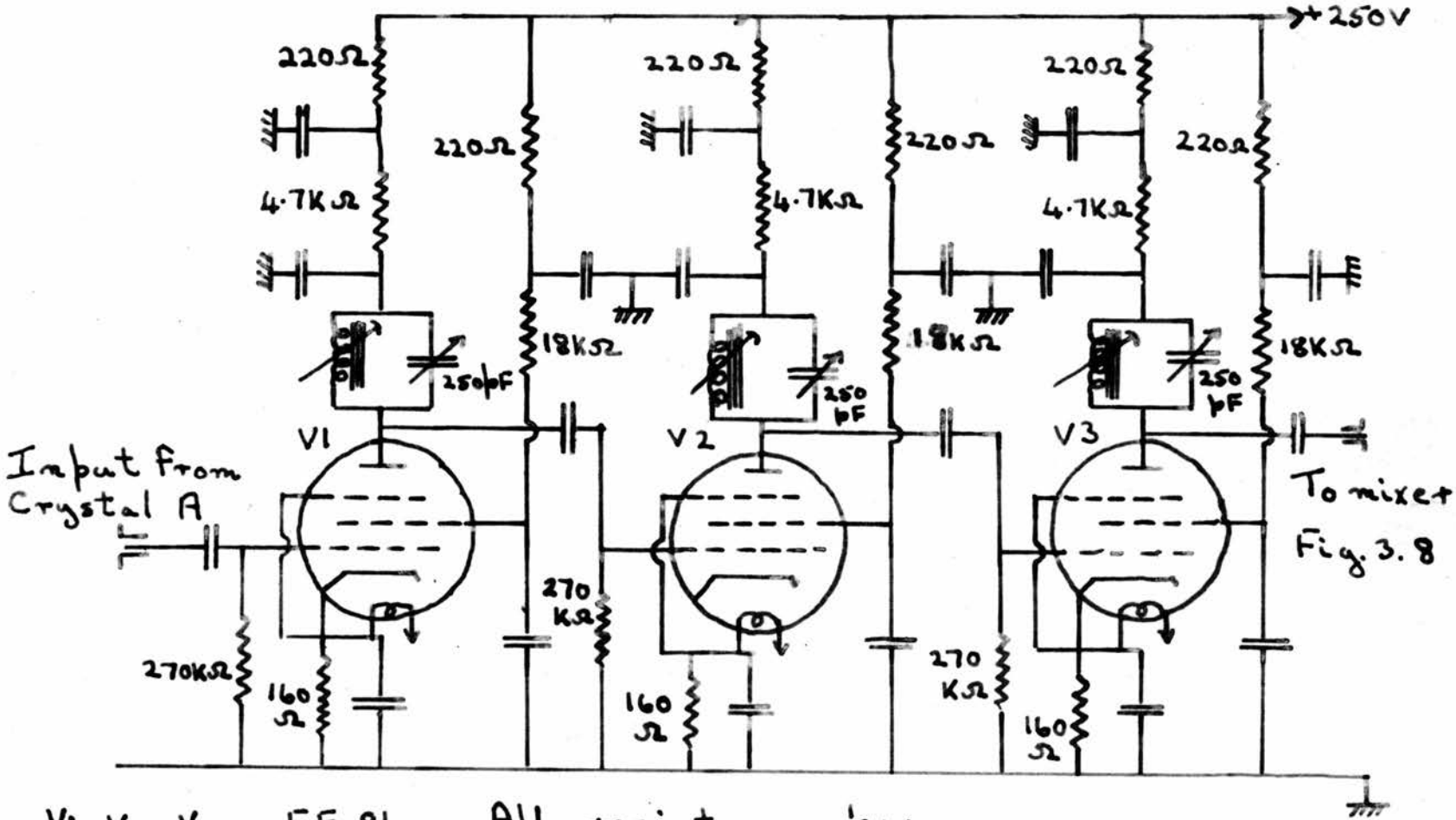

V_1, V_2, V_3 EF 91 All resistors $\frac{1}{2}$ W

Heaters 6·3V A.C. All condensers 0.01μF unless stated.

Fig. 3.7 5 Mc/s Amplifier

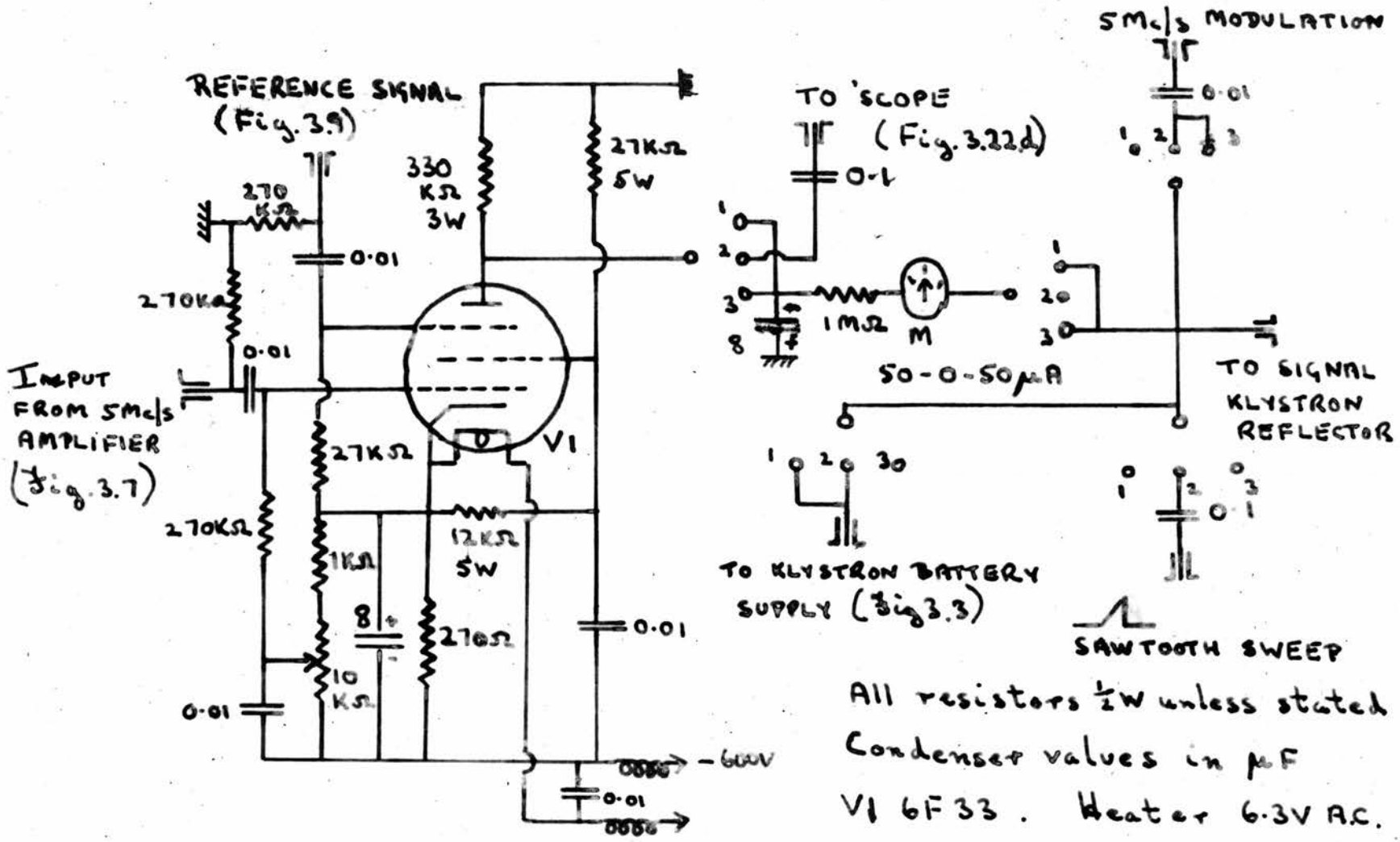

All resistors ½W unless stated
Condenser values in μF
V1 6F33. Heater 6.3V A.C.

Fig. 3.8 5Mc/s Mixer and Stabilisation Control Circuit.

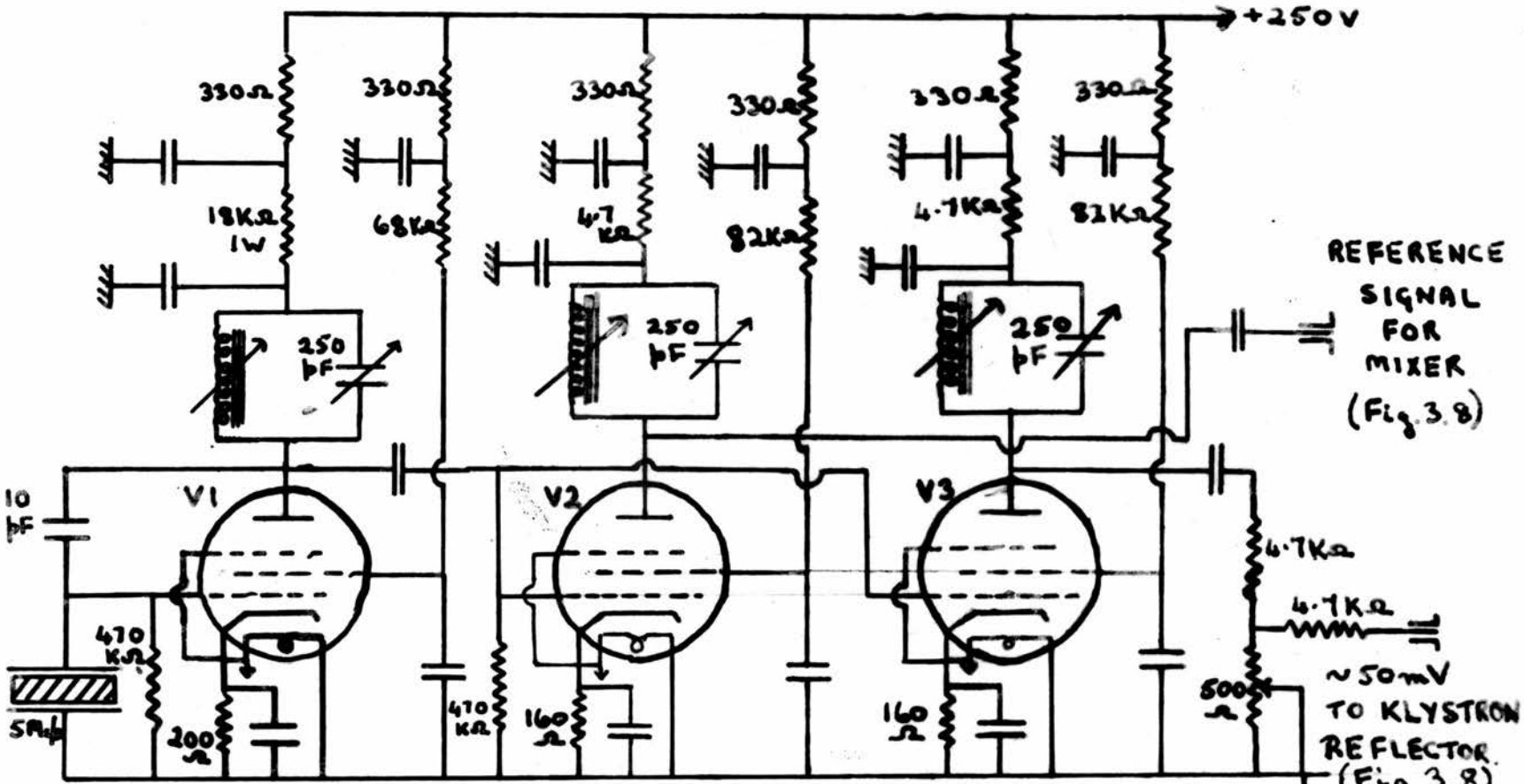

V1 6AK5 All resistors ½ W unless stated Heaters 6·3V AC.

V2, V3 EF91 All condensers 0·01 μF unless stated Crystal G.E.C. Type BA/329

Fig. 3.9 5Mc/s Oscillator and Buffer Stages.

is such as to pull the klystron back to the resonant frequency of the cavity should any difference tend to arise. To do this effectively the voltage correction should be large enough. The correction curve for the whole cavity mode may be viewed by sweeping the klystron through the cavity resonance with a low-frequency saw-tooth sweep and viewing the mixer output on the oscilloscope (Fig. 3.22 (d)). The curve is S-shaped, the maximum and minimum of the curve occurring at the points of inflexion of the cavity resonance. If we assume the cavity to have a Q of about 3,000, and we show later that this is a reasonable estimate, the width between these points of inflexion will be about 3 Mc/s. For the correction of any frequency difference between the incident power and the cavity resonance the gradient of the correction curve in the central region between the points of inflection should be at least as great as the gradient of the reflector voltage/frequency curve for the klystron (Fig. 3.6). This gradient is 0.67V/Mc/s. This requires our peak-to-peak correction curve amplitude over the 3 Mc/s to be at least 2V. We planned for ten times this value to make the stabilisation really effective. The klystron mode display at crystal A (Fig. 3.22(a)) shows that the maximum voltage of this curve, feeding into the high input of the oscilloscope is about 50 mV. If we assume a typical crystal forward resistance of 400ohm this means that the incident power at the crystal for frequencies at either side of the cavity resonance

is about 5 μW, frequency modulated at 5 Mc/s.

If a point of maximum inflection of the resonance curve coincides with the klystron frequency, 100 mV reflector modulation will produce about 1 mV peak-to-peak amplitude of 5 Mc/s signal at the crystal. This figure is derived from consideration of the curve of Fig. 3.22(a) together with a knowledge that the gradient of the frequency/voltage curve for the K302 klystron is 1.5 Mc/s/V If we assume a nominal mixer gain of 10, we see that amplification of about 1,000 is required before the correction signal is as large as we require it to be between the points of inflexion. We chose a three-stage tuned amplifier which proved more than adequate (Fig. 3.7). We could obtain a peak-to-peak signal of about 70V, (Fig. 3.22(d)).

The stabilisation may be brought into operation by use of the switch S, (Fig. 3.8). Position 1 is the position of no stabilisation; no 5 Mc/s modulation is applied to the reflector, which is connected both to the battery supply (Fig. 3.3) and, through centre-zero meter M, to the mixer anode. Variation of the variable resistor in the grid-cathode circuit equalises the battery and mixer anode potentials. In position 2, modulation is applied to the reflector and the low frequency saw-tooth sweep is superimposed to take the klystron through the whole of the operational mode. The control loop is broken, the

reflector voltage coming from the battery supply, and the output of the mixer valve displayed on the oscilloscope. The S-shaped correction curve can have a peak-to-peak value of 70 to 80V, (Fig. 3.22 (d)). In position 3, the stabilisation position, the reflector of the klystron is switched in to the control circuit only, and the variable resistor is used to tune the klystron in to the correct frequency. In operation this system has proved extremely effective. Stability can be maintained for long periods, the only causes of failure being sudden mains fluctuations or microphonics caused by mechanical disturbance. When fine tuning of the cavity with a quartz rod was employed the klystron was observed to correct for slight detuning caused by movement of the rod into and out of the cavity. We can say that the klystron frequency is stabilised in frequency to at least 1 part in 10^4, probably better.

The correct setting of the signal klystron may be judged in any one of several ways.

(1) The wavemeter may be set to the resonant frequency of the cavity, (Fig. 3.22(a)) and a maximum and constant wavemeter detector current obtained after correct setting of the stabilisation controls.

(2) The I.F. amplifier detector current shows a minimum.

(3) The low frequency (50 c/s and magnetic modulation) components of the I.F. amplifier detected output

show a minimum (Fig. 3.22(f)). Viewed on the oscilloscope at maximum oscilloscope gain this output should be a straight line showing R.F. noise components only.

(4) On phase-sensitive detection the output of the 285 c/s narrow band amplifier (Chapter 3.(h)) shows a very sharp minimum. This indication is the most sensitive of all.

The choice of modulation frequency is by no means arbitrary. Too high a frequency will result in modulation broadening from the frequency modulation of the klystron output. This is harmful to the study of narrow absorption lines. The frequency 5 Mc/s should yield overall broadening of 3 gauss (± 1.5 gauss). This might be expected to produce a difference in the appearance of a video DPPH signal. No difference in width could be detected between DPPH lines recorded with and without klystron stabilisation. This can be explained on the basis of the Lorentzian shape of the line, whose overall width is large though the bandwidth is small. The outer regions of the line are indistinguishable from the noise. One might expect that any broadening could be detected using phase-sensitive detection. However, with no stabilisation it was found to be impossible to hold the klystron to the cavity resonance frequency to record an accurate spectrum. 5 Mc/s as frequency was chosen

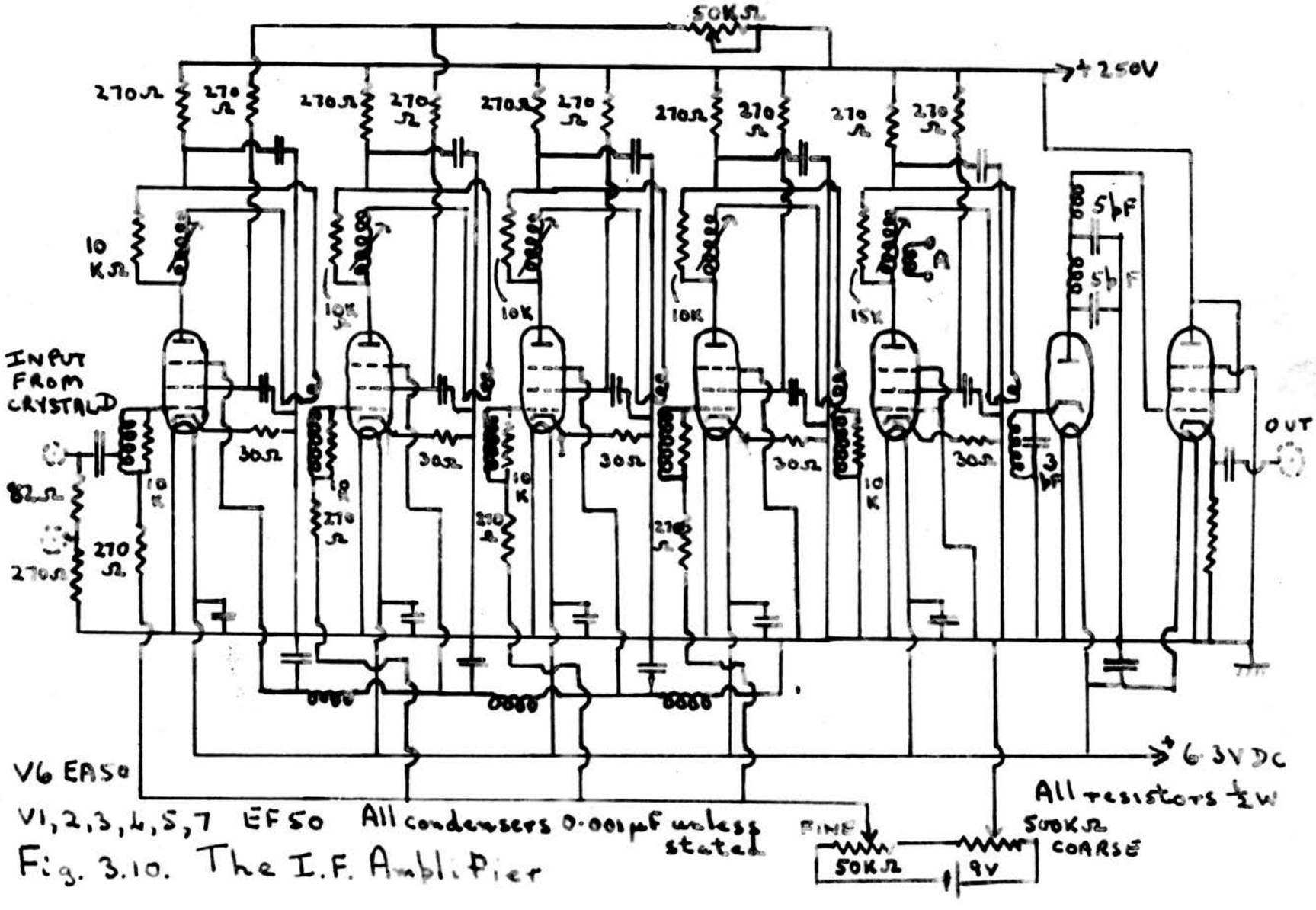

Fig. 3.10. The I.F. Amplifier

because difference components between the I.F. frequency and 5 Mc/s lay without the pass-band of the I.F. amplifier and produced little broadening of the type of lines we expected.

(vi) The I.F. Amplifier

The amplifier was a Services radar-surplus I.F. amplifier, "Pye-strip", of centre frequency 45 Mc/s and bandwidth 10%. The circuit is shown in Fig. 3.10 and consists of a low-impedance input and five staggered-tuned pentod amplification stages, followed by a diode detector and low-impedance cathode follower output stage. Gain control may be exercised by coarse and fine variation of the grid potentials of the first four stages using a 9V grid-bias battery, or by variation of the screen potentials of the first two stages. The gain of the amplifier is at least 50 db at saturation point, but could not be checked exactly by any apparatus available in the laboratory.

A great deal of 50 c/s output modulation was obtained from this amplifier when A.C. heater voltage was used, so five Ni-Fe cells in series were used to heat the valves, with substantial improvement. With the correct setting of all controls of the spectrometer the amplifier output contained less than 5 mV peak-to-peak 50 c/s modulation. Radio-frequency noise in the output may be cut down by passing it through a step R.F. filter with cut-off frequencies 10, 5, 3 and 1 kc/s.

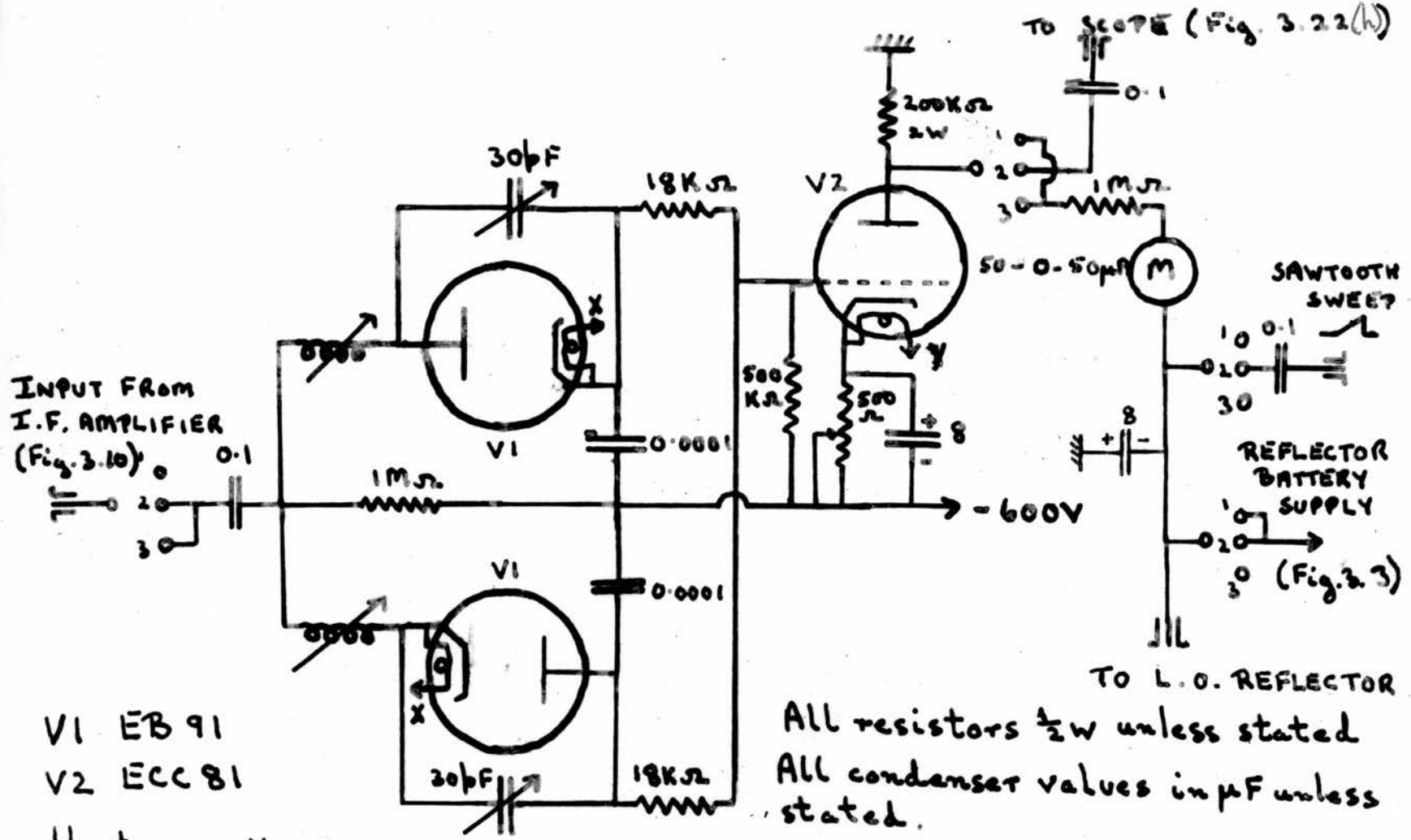

V1 EB 91
V2 ECC 81

Heaters X 6·3V A.C.
Y 6·3V A.C.

All resistors ½w unless stated.
All condenser values in μF unless stated.

Fig. 3.11. Discriminator and A.F.C. Control Circuit

The amplifier has developed component faults from time to time which have proved difficult to trace. It would be to advantage to replace it with a modern amplifier.

(vii) Automatic Frequency Control

Stabilisation of the signal klystron only is by no means enough when superheterodyne detection is used. The frequency of the local oscillator output must be kept at 45 Mc/s less, or greater than that of the signal klystron so that constancy of the I.F. gain and quiescent output is maintained. The method of control employed is again the application of a correction voltage to the klystron reflector.

A small auxiliary coil of 4 turns was wound on the coil-former A of the anode circuit of the final stage of the I.F. amplifier. The signal from this coil was then fed into the discriminator and control circuits shown in Fig.3.11. The two resonating circuits in the discriminator circuit resonate one above and one below the correct intermediate frequency, and D.C. potentials are developed across the diode output condensers of magnitude and sign depending on the difference between the input frequency and the correct intermediate frequency. These voltages are fed direct to the grid of the control circuit which is a D.C. triode amplifier stage whose anode potential may be varied close to the reflector potential by a variable cathode-bias resistor. Control is effected

in much the same manner as with the signal klystron stabilisation scheme by use of the switch S. Position 1 is used for equalisation of battery and control circuit potentials with no signal being fed to the discriminator. In position 2 the control loop is broken, the reflector is at battery potential and the application of a low frequency saw-tooth sweep to either signal or local oscillator klystron reflector will show, on the oscilloscope, the correction curve of form similar to the signal klystron stabilisation curve. (Fig. 3.22(h)). The frequency separation between the peaks of this curve is about 2 Mc/s and a similar analysis as was carried out for the minimum peak-to-peak voltage value for the signal klystron stabilisation showed this value to be 1.5V. With the arrangement described the peak-to-peak voltage of the correction curve varies with I.F. gain. A better arrangement would be to use a suitable pre-amplifier of fixed gain whose input is in parallel with the I.F. amplifier and whose centre frequency is the same thus making the AFC response independent of I.F. amplifier gain. Several pre-amplifiers were tried, but all proved to have insufficient gain, and an attempt to modify an old I.F. amplifier was abandoned because its centre frequency was not quite equal to that of the I.F. amplifier, the AFC in this case holding the frequency difference a little away from the frequency of maximum I.F. gain. However, the arrangement used above has proved satisfactory for all I.F. gains used, peak-to-

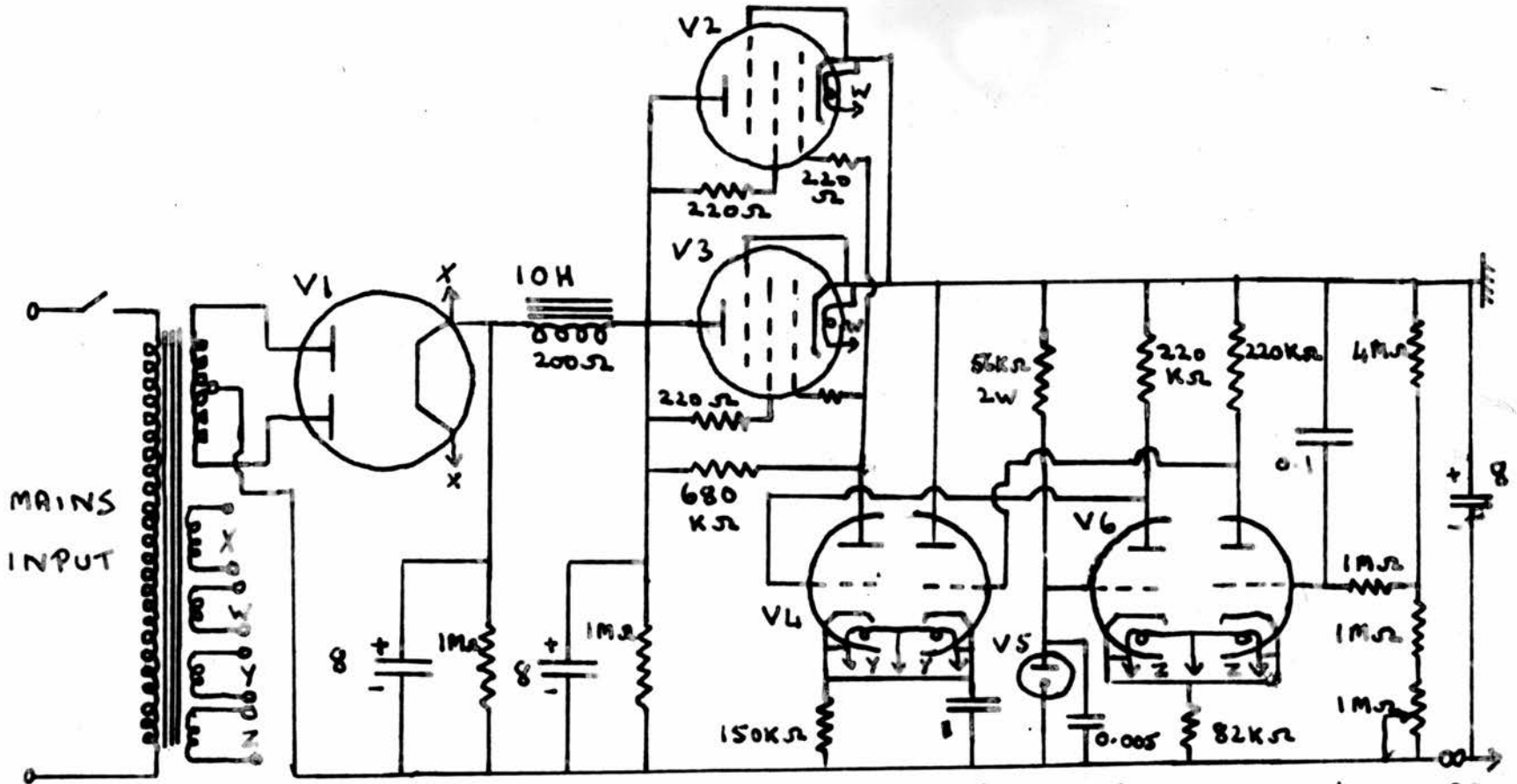

V1 5U4G V4,V6 6SL7 All resistors ½W unless stated

V2,V3 EL84 V5 85A2 All condenser values in μF.

Heaters X 5V A.C. ; W, Y, Z 6.3V A.C.

Fig. 3.12 Stabilised Power Supply 0 → -350V

peak correction voltage at maximum I.F. gain being about 50V.

In switch postion 3, the control position, the klystron reflector is connected only to the anode of the control valve and its potential is varied until the desired point of operation is reached, this point being judged by video display of the I.F. amplifier output and by the indicated second detector current.

The I.F. amplifier will remain on the centre frequency for long periods with this AFC arrangement, the main causes of failure being mains surges and mechanical disturbance, or sudden failure of the signal klystron stabilisation scheme.

(viii) Power Packs

Five stabilised power supplies have been used. The circuit of 0 → - 350V klystron anode - cathode supply is shown in Fig. 3.12. All the other supplies are built on the same principle, though using different transformer secondary voltages, chokes, component values, neon tubes and numbers of series valves. All these supplies gave an output 50 c/s ripple, on load, of less than 5 mV, peak-to-peak. The power packs with the circuits they supply are:-

(1) 0 → - 350V; anode-cathode voltage for both klystrons. (See Fig. 3.3)

(2) 0 → - 600V; supply for the signal klystron stabilisation control circuit, originally designed as a floating supply but modified because of earthing troubles.

(3) 0 → - 600V; AFC control circuit supply.

(4) 0 → 250V; supply for 5 Mc/s oscillator and tuned amplifier, I.F. amplifier, 285 c/s narrow-band amplifier and phase-sensitive detection and recording circuits.

(5) 0 → 250V; built by Mr. I. M. Brown, supply for 285 c/s oscillator, buffer amplifiers and power amplifier.

(ix) The Mounting of Microwave and Electronic Equipment

A rectangular frame, 1¼ ft. x 3 ft. x 5 ft. high, constructed of "Handy Angle" was screwed to the concrete floor. The electronic apparatus was mounted on the front and back sides of this frame on vertical tinned-iron chassis with the valves, transformers, chokes and large condensers pointing to the inside and the soldered components on the outside face. This arrangement makes for simple access in servicing. The power-packs were mounted at the rear of the frame, and the rest of the electronics with all meters and controls at the front (Fig. 3.1). Other items such as H.T. batteries and some heater transformers were mounted on horizontal shelves within the frame and the many interconnecting coaxial leads clipped along the sides of the frame.

The main microwave bridge is mounted on stands on a ½ in. horizontal wooden board screwed down on top of the frame.

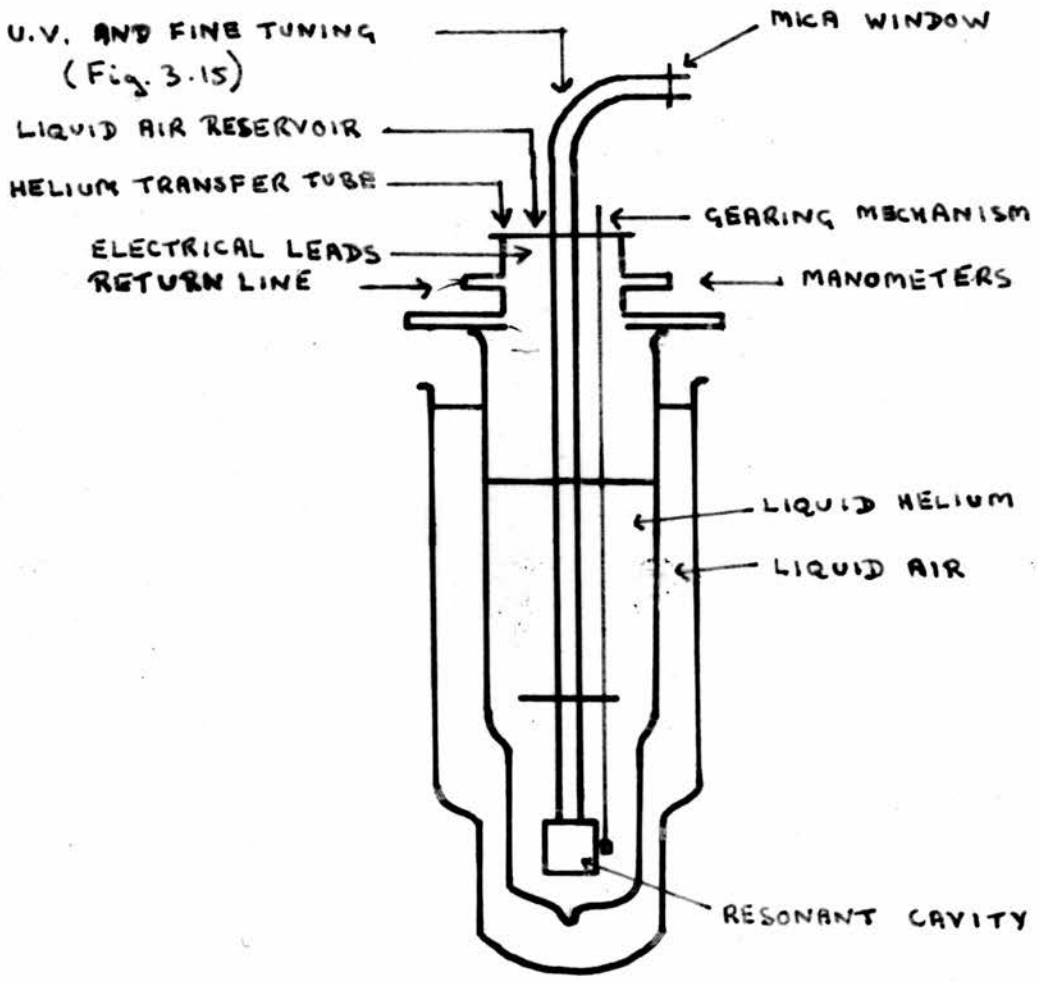

Fig. 3.13. The Cryostat (Schematic)

(3.c) The Cryostat

A schematic diagram of the cryostat is shown in Fig. 3.13. It is mounted on the front of a rectangular bridge frame of "Handy Angle" which spans the rails on which the magnet trolley runs. The frame dimensions are 3 ft. x $1\frac{1}{4}$ ft. x $5\frac{1}{6}$ ft. high (Fig. 3.1). The main brass supporting plate of the cryostat, 8 in. x 6 in. x $\frac{1}{4}$ in., rests on four OBA levelling screws fixed to a horizontal platform consisting of two lengths of "Handy Angle" bolted to the top of the bridge and protruding 6 in. in front of it, (Fig. 3.15). The cryostat may be lowered into position over these screws and is held down by four wing-nuts fitting on the screws. A brass cylinder, of inner diameter $2\frac{3}{8}$ in., is set through the centre of this main supporting plate, and protrudes $\frac{1}{4}$ in. down from the lower side of the plate. The inner Dewar vessel slides over this cylinder beneath the main plate against a Gaco ring, and is held in position by a brass disc which slips over the outside of this Dewar, pressing a Gaco ring against the bottom of the Dewar lip, and held against the main plate by three symmetrically placed OBA screws, which are screwed in to finger tightness. As this Dewar is evacuated it is pulled up more tightly against the top Gaco ring and these screws are again screwed to finger tightness.

Three openings to the cryostat protrude from the cylinder above the main plate. The first is a 1 in. inner diameter copper pipe

leading to a 1 in. Saunders valve capable of shutting off the cryostat from the return and pumping lines, which can be broken at a join just to the left of this valve before the cryostat is taken off its support, (Fig. 3.14). The second opening is a brass tube of inner diameter $\frac{1}{4}$ in. to which can be fitted a rubber vacuum tube leading to a $\frac{1}{4}$ in. flexible metal tube which itself leads to the manometers, mounted on the left-hand side of the cryostat supporting frame, (Fig. 3.1). The third opening at the rear of the cylinder is for electrical connections and is a tube of $\frac{1}{4}$ in inner diameter terminating in a vacuum-to-air electrical connector with six terminals. Two of these terminals only have been used until now for a heater wire of insulated Eureka, 32 SWG, which is used to boil off the helium at the end of a run. The wire is led down to a point just above the level of the cavity where it is wrapped round the waveguide several times and fixed down with nail varnish. It is held down to the waveguide leading to the top by loops of thread (Fig. 3.5(a)). The resistance of this wire is about 30 ohm. and it is supplied by a 6V secondary mains transformer.

The top cap of the cryostat is set into the top of the cylinder over a Gaco O-ring and is screwed down by six 2 BA screws round its circumference (Fig. 3.15). The waveguide bend leading from the microwave bridge down into the cryostat enters the top cap through a bush of standard British-size 3 cm. waveguide, whose inner

dimensions 1.000 in. x 0.500 in. are the same as the external dimensions of the waveguide leading into the cryostat. This bush is set into the centre of the top cap. The thin-walled waveguide is fitted into a filed-out bush of American-size waveguide which is itself fitted into the larger bush until it butts against the end of the incoming waveguide. The join is then soft-soldered.

The broad face of the cryostat waveguide runs parallel to the magnet poles when the magnet is facing to the front of the apparatus.

Several other openings are set in the outer area of the top cap. One is to take the liquid helium transfer tube at the liquefier which must protrude right down almost to the tail of the inner Dewar. A guide tube 18 cm. in length for this transfer tube is soldered to the cryostat waveguide. At all other times this exit is sealed off by a rubber bung. This will be blown out under any over-pressure and there should be no danger of an excessive build-up of pressure occurring during the course of a helium run.

A second opening is used as the exit tube of a small reservoir made from $\frac{1}{2}$ in. diameter copper-nickel tubing whose bottom makes good thermal contact with the thin-walled waveguide at a point 7 in. below the level of the top cap. If this reservoir is kept filled with liquid air during the course of a run, the 83°K point along the cryostat waveguide is raised and the heat leak should be lowered. In practice it was found that use of this reservoir did not

appreciably increase the running time which has been extended on several occasions to twelve hours without use of the reservoir.

A third opening is for the turning rod of the cavity gearing mechanism. The rod passes tightly through a rubber disc of diameter $\frac{1}{4}$ in. which is held down flat on the opening by a screw cap, through which the rod protrudes to the knurled turning knob. There are two other openings in the top cap not at present in use, but kept sealed.

All openings and metal joints at the top of the cryostat are carefully brazed or soldered to prevent leaks under vacuum.

(3.d.) The Dewar Vessels

Both Dewars were made from commercially obtained cylindrical moulds of "Monax" glass. They were made and pumped in the laboratory. The dimensions of the Dewars are indicated below.

HELIUM DEWAR

Tail	Wall thickness	= 0.5 mm.
	Inner wall	= 34.5 mm. O.D.
	Outer wall	= 37.5 mm. O.D.
	Length	= 20 cm.
Main Body	Wall thickness	= 1-2 mm.
	Inner wall	= 55.5 mm. O.D.
	Outer wall	= 69.0 mm. O.D.
	Single walled top (length)	= 12 cm.

Overall Length		= 70.5 cm.
Capacity		1 litre.

AIR DEWAR

Tail	Wall thickness	= 0.5 mm.
	Inner wall	= 40.5 mm. O.D.
	Outer wall	= 44.5 mm. O.D.
	Length	= 21.5 cm.
Main Body	Wall thickness	= 1-2 mm.
	Inner wall	= 89.5 mm. O.D.
	Outer wall	= 101.5 mm. O.D.
Overall Length		= 61.3 cm.

The Dewar vessels are shown in position between the magnet pole pieces in Fig. 3.16. The outer Dewar is held in a cage consisting of a horizontal ring collar with three vertical 4 BA screwed rods, which passes over the outer Dewar, holding it by a rim in the Dewar 10.5 cm. below the top. The vertical 4 BA screwed rods pass through symmetrically placed holes in the top cap and are held by nuts.

It was found necessary to repump the Dewars, which were used also at another experimental station, after ten or twelve helium runs.

(3.e.) The Pumping System

A schematic diagram of the plumbing leading to the cryostat is shown in Fig. 3.14. The whole cryostat may be uncoupled from this

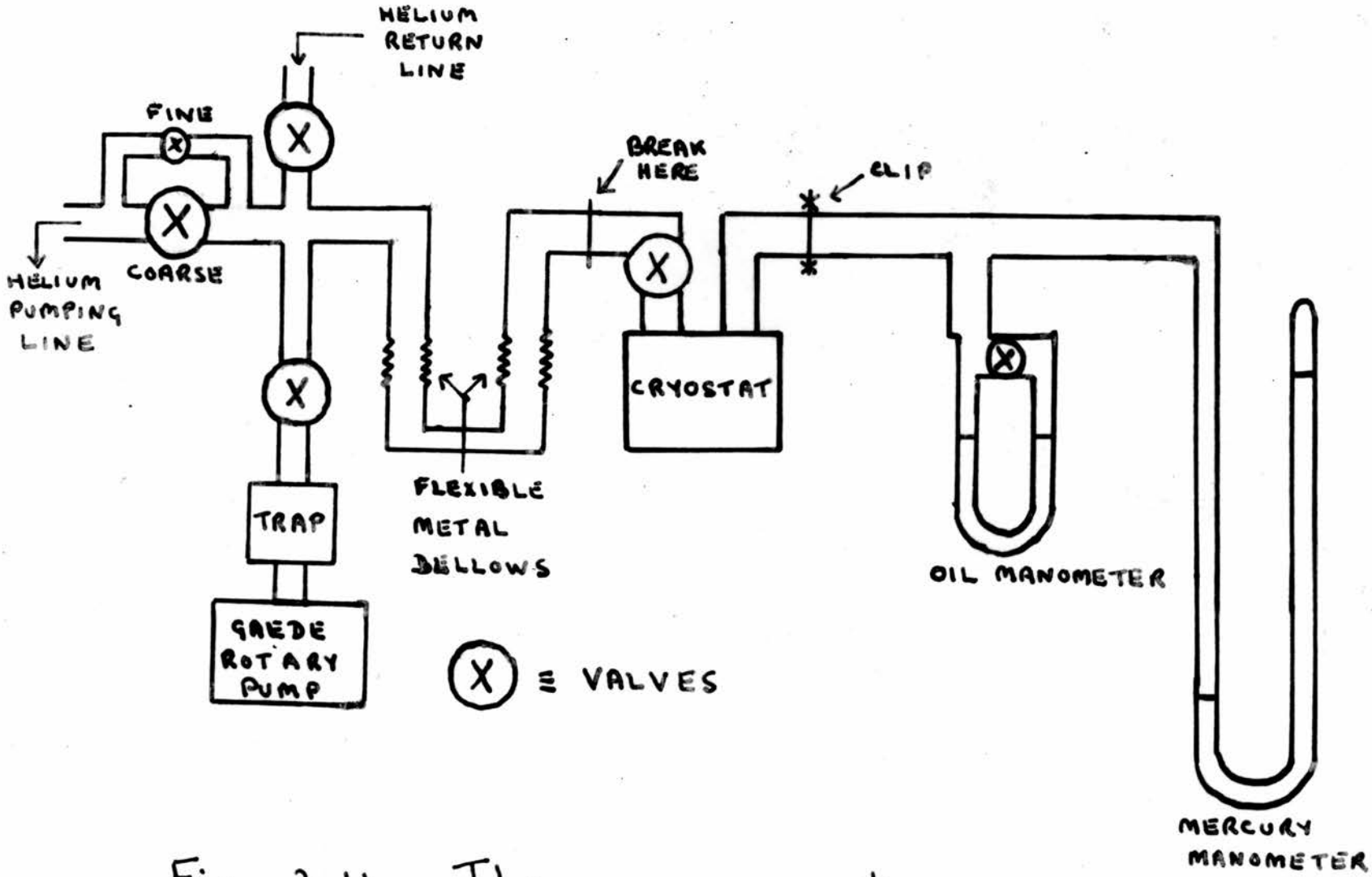

Fig. 3.14. The vacuum system

line at a point just to the left of the 1 in. Saunders valve at the top of the cryostat. The flexible metal bellows arrangement prevents vibrations from the 2 in. helium pumping line from reaching the cryostat.

On normal operation at 4.2°K the cryostat is opened to the helium return line, a ½ in. diameter copper tube leading to the gasholders. To lower the temperature below 4.2°K the return line valve is closed and the pumping valves, fine and coarse, slowly opened so that the pressure in the cryostat goes down very slowly. The temperature may be deduced by reading the mercury manometer and using liquid helium vapour pressure tables, (V1). The lowest limit obtainable with our pumps is about 1.2°K. A needle valve was inserted for the fine control but in practice it was found that the Saunders valve was more effective for fine control.

Before a helium run the cryostat is evacuated by a Gaede rotary vacuum pump which is kept running for about one hour to ensure that all water vapour is removed. The leak into the cryostat is less than 0.25 cm. of mercury pressure per hour. The outer Dewar, held by its rim in the cage already described, is filled with liquid air, and helium gas at atmospheric pressure is admitted to the cryostat from the return line an hour or two before the liquid helium is expected. When the cryostat is to be carried to the liquifier the 1 in. Saunders valve at the head of the cryostat is

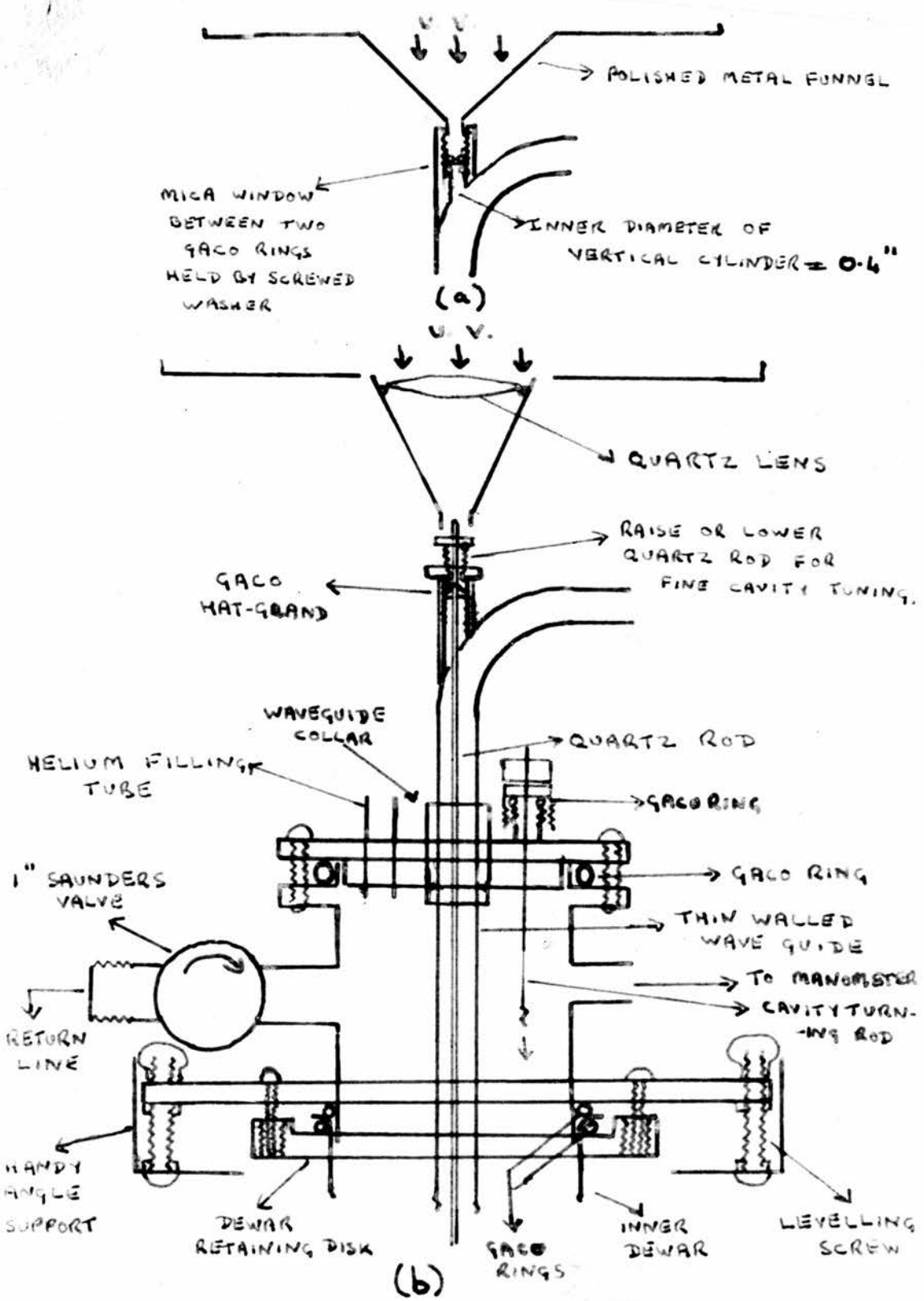

Fig. 3.15. a) New arrangement for u.v. illumination
NOT TO SCALE b) Old arrangement for u.v. illumination using quartz rod as light pipe and tuner

closed, and the manometer lead slipped off and clipped, its entrance tube being closed with a rubber bung. All electrical microwave and mechanical connections are then broken and the cryostat carried to the liquifier. On the trip back helium gas must be allowed to escape into the air until the cryostat can be connected into the return line. With practice the time of loss has been cut below two minutes.

(3.f.) Ultra-violet Illumination of the Specimens

The two arrangements used for illuminating the specimens are shown diagramatically in Fig. 3.15, together with a rough diagram of the top portion of the cryostat.

In the first arrangement a quartz rod of diameter 3 mm. protruded through the hole in the broad face of the waveguide bend at the top of the cryostat, down the centre of the waveguide and a few mm. into the cavity where its central alignment was maintained by a thin circular mica disc, with a 3 mm. central hole, stuck to the top face of the cavity with "Vaseline". At the top the rod passed through a Gaco hat-gland, held against the supports round the bend hole by a $\frac{3}{8}$ in. screw. The rod then passed through a hollow $\frac{1}{4}$in. screw, which could be moved up and down inside the $\frac{3}{8}$ in. screw, the distance of travel being about $\frac{1}{2}$ in. The rod was sealed to the inside of the $\frac{1}{4}$ in. screw with vacuum-tight "Araldite Type 1" wax.

Experiments were performed with short glass rods, white light

sources and photocells to find out whether broadening and narrowing of the tips of the rods in any way affected the intensity of light emerging from one end of a rod, when light was focussed on the other end. As a result of these experiments it was clear that the most efficient light pipe of this sort was a simple straight rod, no portion of which had been melted at any time since its manufacture.

The U.V. lamp was mounted in a rectangular box of $\frac{1}{8}$ in. hard-board of dimensions 12 in. x 8 in. x 8 in., which was lined with asbestos paper. The box was ventilated and surrounded with black paper on the outside to prevent U.V. radiation getting out. A 1 in. cylindrical brass tube at one side led to a flexible line leading to an electric air-blower in an outer building. Air from this blower was used for klystron cooling at all experimental stations in the laboratory. The U.V. lamp box was placed on a frame above the cryostat (Fig. 3.1). A quartz lens of diameter $1\frac{1}{2}$ in. and focal length $2\frac{1}{2}$ in. was held against a hole in the foot of the box, on the top of a polished metal cone, the bottom of which was held over the top tip of the quartz rod. In this way light from the box was brought to a focus on the tip of the rod. An arrangement of polished thin aluminium sheeting round the lamp within the box enabled a good deal of reflected light to be incident upon the lens.

No photo-cell was available in the laboratory which was sensitive enough to detect the intensity of the light emerging from the foot of

the rod into the cavity. A good comparative test was devised, however. The bottom face of the cavity was covered with fluorescent anthracene and the bottom half held against the top half in darkness. The positions of lamp, lens and top tip of the rod were then adjusted until the fluorescence showed a maximum.

It was found to be difficult to estimate the intensity of light emerging from the rod. Although a good estimate of the intensity of light entering the rod can be made from a knowledge of the characteristics of the lamp and the geometry of the focussing system, no values of the absorption coefficients of quartzes for U.V. wavelengths could be traced.

After a few helium runs of the sort described in Chapter 4, which did not yield free radical spectra, another arrangement was tried which did transmit much more light into the cavity, as shown by the anthracene test. This arrangement is also shown in Fig. 3.15. The whole quartz rod assembly was removed and a larger hole bored through the waveguide bend. A hollow brass cylinder of inner diameter $^{2}/_{5}$ in. was shaped to the broad face of the bend and brazed on over the hole. A vacuum seal was constructed inside this cylinder using a mica window sandwiched between two Gaco rings and held down against the rim of the cylinder by a screwed washer. Another wider polished metal cone was fitted in on top of the washer and the U.V. lamp shone straight through an enlarged hole in the foot

of the box, into the waveguide and down to the cavity. The inner walls of the waveguide were well polished. The inner diameter of the cylinder mounting was chosen so that waves of frequency 9375 Mc/s should be evanescent within it. In practice the presence of this large hole in the broad face of the waveguide bend made no appreciable difference to the shape and intensity of the cavity mode display (Fig. 3.22(a)), so it is assumed that the sensitivity is not impaired thereby, since little energy is reflected or removed by the discontinuity.

The lamp used is an Hanovia quartz medium-pressure Hg arc source, type U.V.S. 500, with a U-shaped tube type 506/6, the U pointing down towards the cryostat. The total wattage of radiant energy in the U.V. range is claimed to be 52 W.

This arrangement has also failed to produce large enough concentrations of radicals to be detectable with our equipment. The experiments are discussed in Chapter 4.

(3.g.) The Magnet

(i) General

The electromagnet was designed by members of this Department in collaboration with Newport Instruments, Ltd., and was built by that firm. They have since adapted it as a standard 7 in. magnet Type E.

The magnet and trolley are shown in Fig. 3.16 with the Dewars

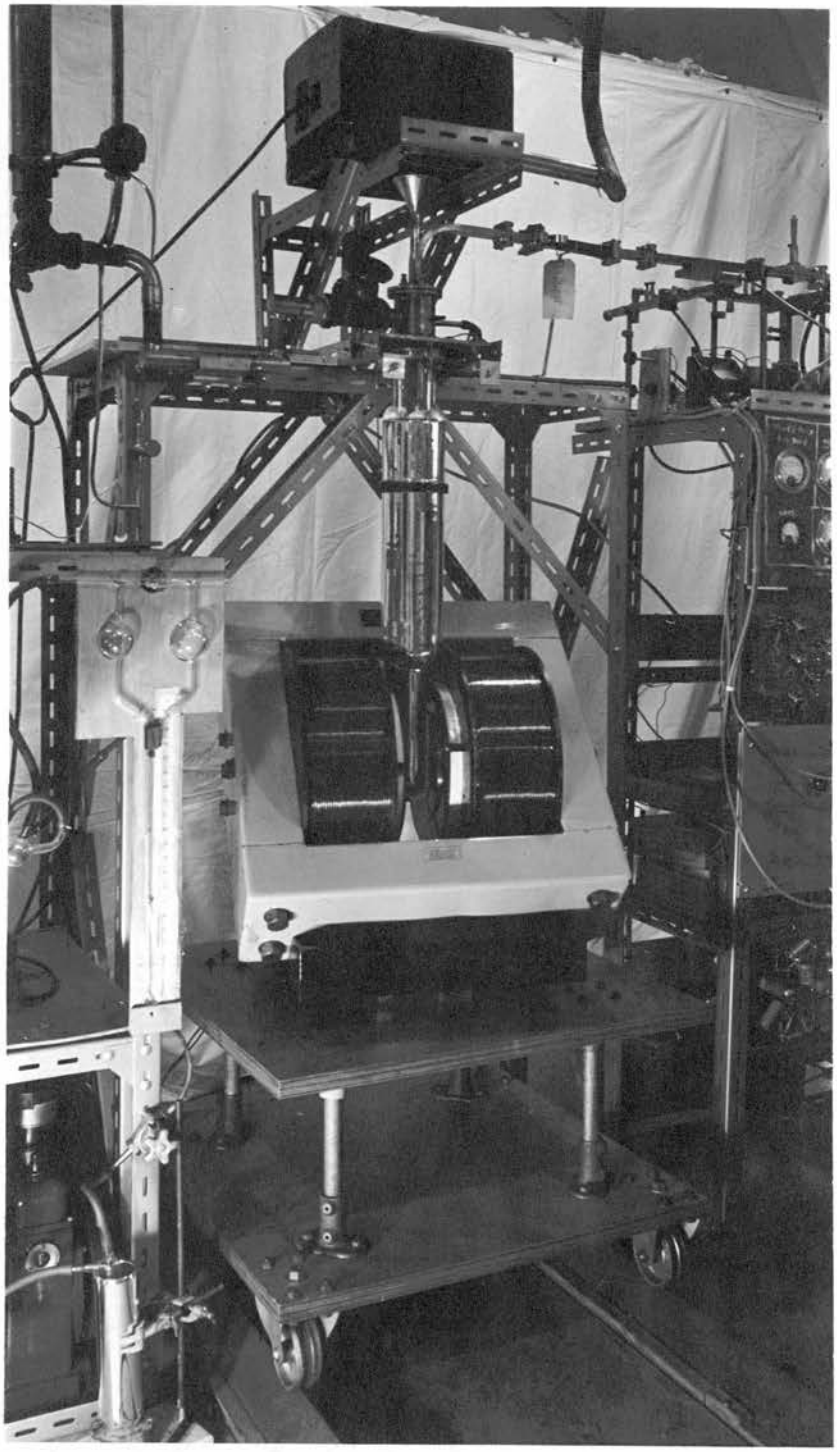

Fig. 3.16. The Magnet and Cryostat.

mounted between the pole-caps. The yoke is mounted at an angle of 45° on the support, which revolves on a set of roller bearings set in a circular groove in a circular steel plate bolted to the wooden trolley. The outer rim of this plate is graduated in degrees so that the angle of the magnet relative to the forward position can be set eaily, if it is required to take any measurements with the magnet at different angles. Also, since the magnet is shared between three experimental stations, it must be rotated through 180° to get it past any one station, because of the cavity arm, which protrudes down as far as the centre of the magnet gap. The trolley is mounted on grooved cast iron wheels, on 4 in. angle-steel rails set 30 in. apart on the level floor, and its top was carefully levelled before mounting the magnet.

The magnet yoke, in four sections of cross section $3\frac{1}{2}$ in. x 7 in., is of closed construction and is made of best quality Grey Cast iron. When the four sections are bolted together with $\frac{3}{4}$ in. steel bolts the height and breadth are each 23 in.

The pole pieces of mild steel are milled flat and parallel, (tolerance ± 0.0005 in.), and are each bolted to the side pieces of the yoke by three $\frac{1}{2}$ in. steel bolts. The pole caps are ground flat to the same tolerance and are each held by a single $^{7}/_{16}$ in. bolt running through the centre of the pole pieces to the side of the yoke.

The main coils are wound of standard insulated rectangular copper wire of cross-section 0.0075 sq. in., in a total winding space of 5 in. x $3\frac{3}{4}$ in., on brass bobbins of maximum diameter 20 in., which rest on shaped wooden blocks fitted to $\frac{1}{2}$ in. brass plates whose levels may be controlled by levelling screws set in the base plate of the support. There is an air gap of $\frac{1}{4}$ in. between the coils and the pole pieces to help cooling. When the bobbins were set in the correct position they were fixed by brass flanges to the horizontal sections of the yoke. The spacing between the bobbins is $4\frac{3}{8}$ in.

The magnet arrived in its component parts and was assembled on the trolley according to the manufacturers' instructions. The trolley was made in the laboratory. The pole pieces were aligned until uniformity of distance across the gap was achieved to the tolerance of the flatness of the pole-caps. The parallelism was judged using a clock gauge whose minimum graduation is $\pm$ 0.0005. Slight adjustments of the respective positions of the pole pieces were made by slackening the bolts holding the yoke and tapping the yoke components with a rubber hammer.

(ii) Performance Data

Number of turns per coil	= 1,850
Resistance of each coil	= 5.75 ohm.(cold)
Maximum permitted increased over cold value	= 40%
Air gap between pole-caps	= $2^{5}/_{16}$ in.

Field Data	Amps	Volts	Gauss
(Coils connected in	1	12	800
series aiding)	2	24	1,500
	3	35	2,250
	4	46	2,850
	5	58	3,500
	6	68	4,000
	7	80	4,550
	8	91	5,000

Currents up to 8 amps may be used continuously but only intermittent operation is permitted from 8 amps to 10 amps. For free radical investigations at 9375 Mc/s the field is between 3,000 and 3,600 gauss.

(iii) Sweep Coils

Two pairs of sweep coils have been used. The first pair were wound on brass bobbins made in the laboratory. 2,900 turns of insulated 26SWG copper wire were wound on those bobbins whose winding space was insulated by insulating paper stuck down with "Bostic". The wire was wound on with the help of a slowly turning lathe. These coils produced roughly the right order of sweeps desired, but were very noisy both acoustically and from the point of view of microphonics.

The pair of coils which has replaced the above has been made for

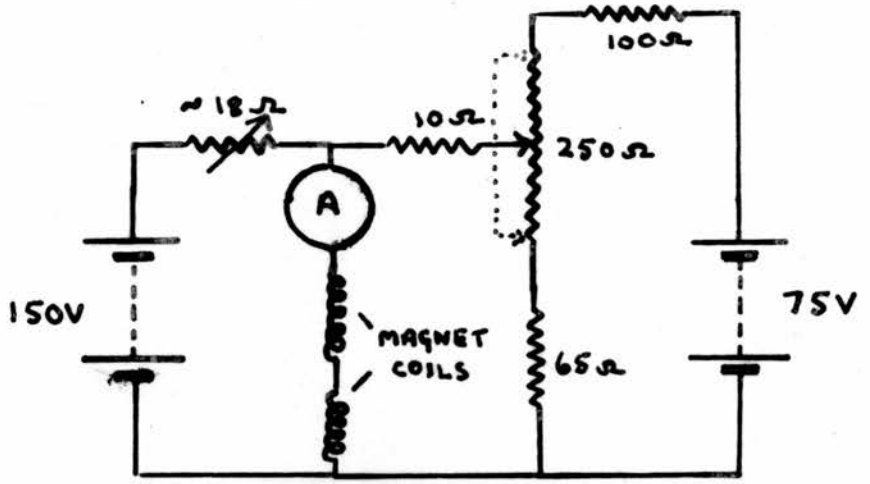

(a)

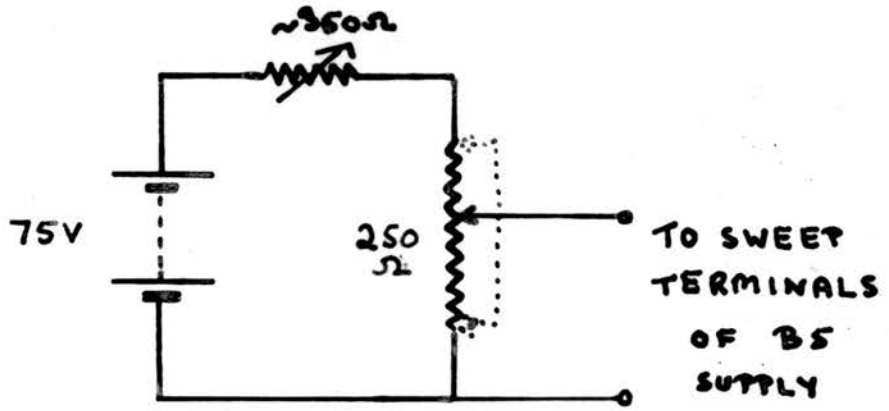

(b)

Fig 3.17. D.C. slow sweep circuits
a) With battery current supply
b) With BS power supply

the magnet by the Newport Company. These Type E coils have 3,500 turns each, are wound on bakelite formers and are far less noisy.

The coil-formers of both these pairs of sweep coils were screwed to the side faces of the main bobbins and envelope the pole-caps almost to the level of their faces.

(iv) Magnet Current Supply

Until a few weeks before writing, the magnet current was drawn from a bank of 12V lead accumulators, 12 in all. These cells could be used as two banks of 75V each, or as one of 150V, and the current was controlled by a series of rheostats progressively lower in resistance value and graded in current up to a maximum of 12.5A. The batteries were charged at currents up to 6A through a rectifier which could be connected in to trickle charge while the magnet was drawing current. This arrangement suffered from the disadvantage that the field could not be held steady because the battery voltage dropped unless the trickle-charging was at high current, and because the heat capacity of the coils was so high that an equilibrium temperature was never reached even after several hours continuous operation, resulting in a constant change of coil resistance. This arrangement for a slow sweep of current through the main coils is shown in Fig. 3.17(a). The sweep rheostat is driven by a D.C. motor, whose speed may be varied by a "Variac" transformer operating through a rectifier. With this arrangement the sweep was found to be

approximately linear with time at constant motor speed, for sweeps up to 200 gauss. At values above 200 gauss the increase with time was much faster.

Two stabilised current units, Type B5 by Newport Instruments, Ltd., have recently arrived for use in this laboratory. These provide a stable supply of D.C. current up to 12A, 150V. The field ripple claimed is 1 part in 10^5, or 0.035 gauss in 3,500 gauss. Two sweep voltage terminals are incorporated to which a slowly varying voltage may be applied (Fig. 3.17(b)). Whether the change is linear with respect to voltage applied to these terminals is not clear from the specifications received up to the time of writing. However, it was noticed that the current output rose more rapidly when the voltage applied to the terminals rose above 20V. 25V injected voltage gives a current change of approximately 1 amp, corresponding to a field change of about 600 gauss, which is larger than most free radical line widths. The great advantage of these new units over the old arrangements is that the current output is stabilised and is independent of change in magnet resistance.

(v) Homogeneity

After the magnet had been lined up and the pole caps tested for parallelism, measurements of magnetic field were made using a nuclear magnetic resonance method by Lowe (L6). A moveable probe consisting of a small coil immersed in glycerol is fed with energy from a

variable oscillator, and magnetic field is measured by adjusting this oscillator until the nuclear resonance line of the glycerol appears on an oscilloscope. Measurement of field variation for vertical and horizontal travel of the probe parallel to and midway between the pole-caps, and for horizontal travel across the centre of the gap were taken at current values close to the free radical value. The battery supplies were trickle-charged and the magnet run at this current for several hours before measurements were taken. Even then the field drift is considerable, about 0.5 gauss per minute, and drift readings were taken at regular intervals to give correction values for the field readings. The limit of accuracy of the nuclear magnetic resonance equipment is such that the field variation over the first 2 cm. towards the outer regions of the gap lies within this limit. A large number of readings were therefore taken in the region round the centre of the gap, and after plotting the readings on a graph a clear picture of the field variation was obtained, from which it was evident that the field variation within a circle of 2 cm. radius half-way between the faces is not greater than $\frac{1}{2}$ gauss. Variation of field between the faces with both sweep coils running in parallel at 50 c/s or 285 c/s is about 2 gauss. The measurements clearly indicate that the variation within 1 cc. at the centre of the gap is less than or of the order of 0.1 gauss, which is adequate homogeneity for our purpose.

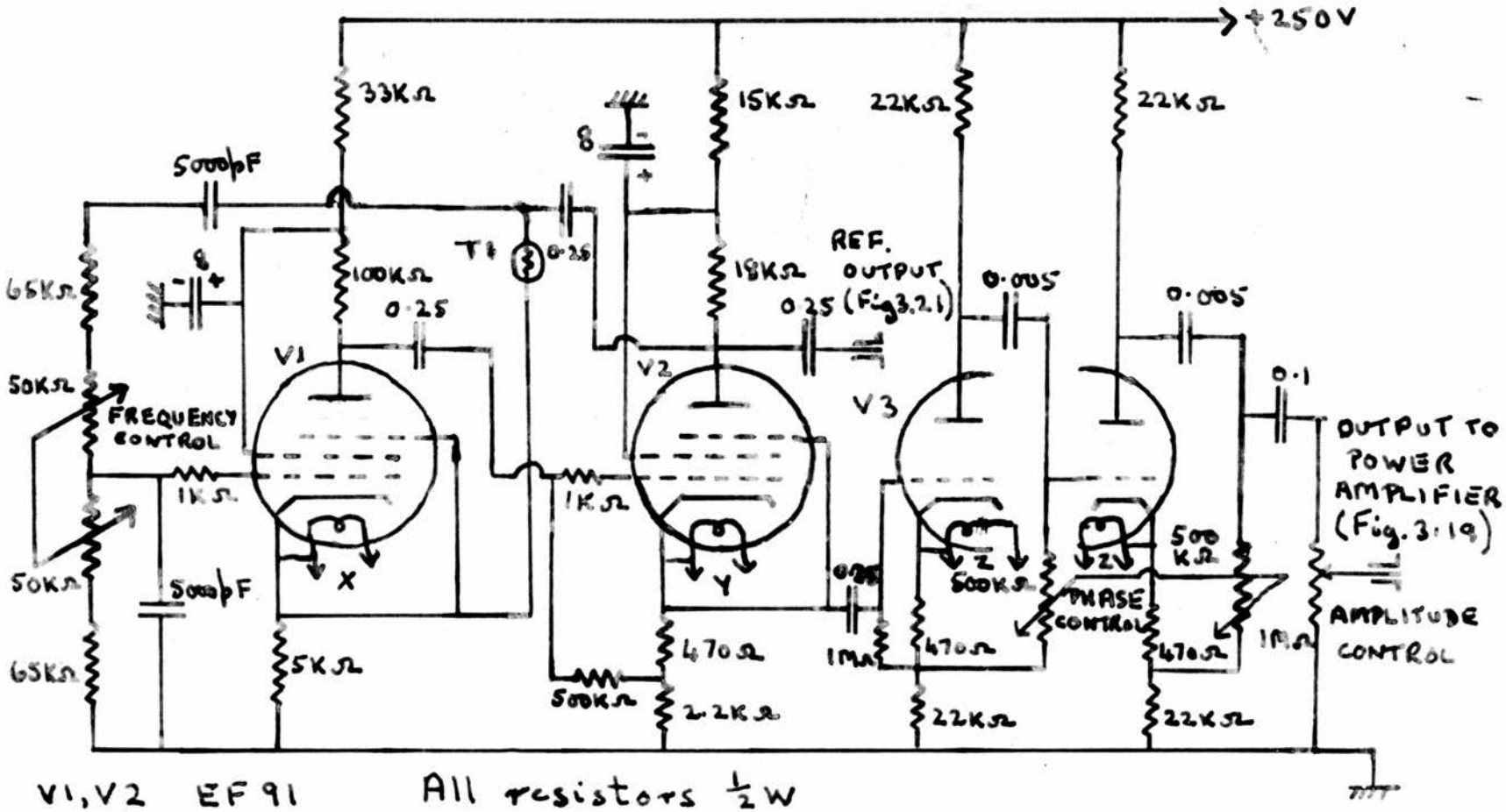

V1, V2 EF 91 All resistors ½ W

V3 ECC 81 All condenser values μF unless stated.

T1 Thermistor A5513 Heaters X, Y, Z 6·3 V A.C.

Fig. 3.18. 285 c/s Oscillator with Buffer Stages.

(3.h.) Phase Sensitive Detection

The principle by which a slow sweep of the magnetic field, together with a small A.C. modulation on auxiliary sweep coils, can be made to record the derivative of a resonance line is described in I1. The principle of phase-sensitive detection is the same as that used in the signal klystron stabilisation scheme where the reflected signal from the cavity is passed through a tuned amplifier and mixed with a reference signal to produce voltages at the anode of the mixer stage dependent on the amplitude and phase of the incoming signal.

Maximum sensitivity of detection is achieved by this method when the magnetic modulation is of the order of the resonance line width, but a true derivative is traced out only when the modulation is not more than $^{1}/_{10}$ the width of the narrowest hyperfine component of the absorption line.

The frequency chosen for the detection scheme was 285 c/s being a low frequency but not a multiple of 50 c/s. Any narrow-band amplifier operating on a multiple of 50 c/s or a harmonic of 50 c/s will amplify the harmonics and multiples of 50 c/s pickup, in addition to the required signal.

The circuit of the oscillator which feeds the power amplifier for the coil modulation and which provides the reference voltage for the lock-in-detector, is shown in Fig. 3.18. This unit and

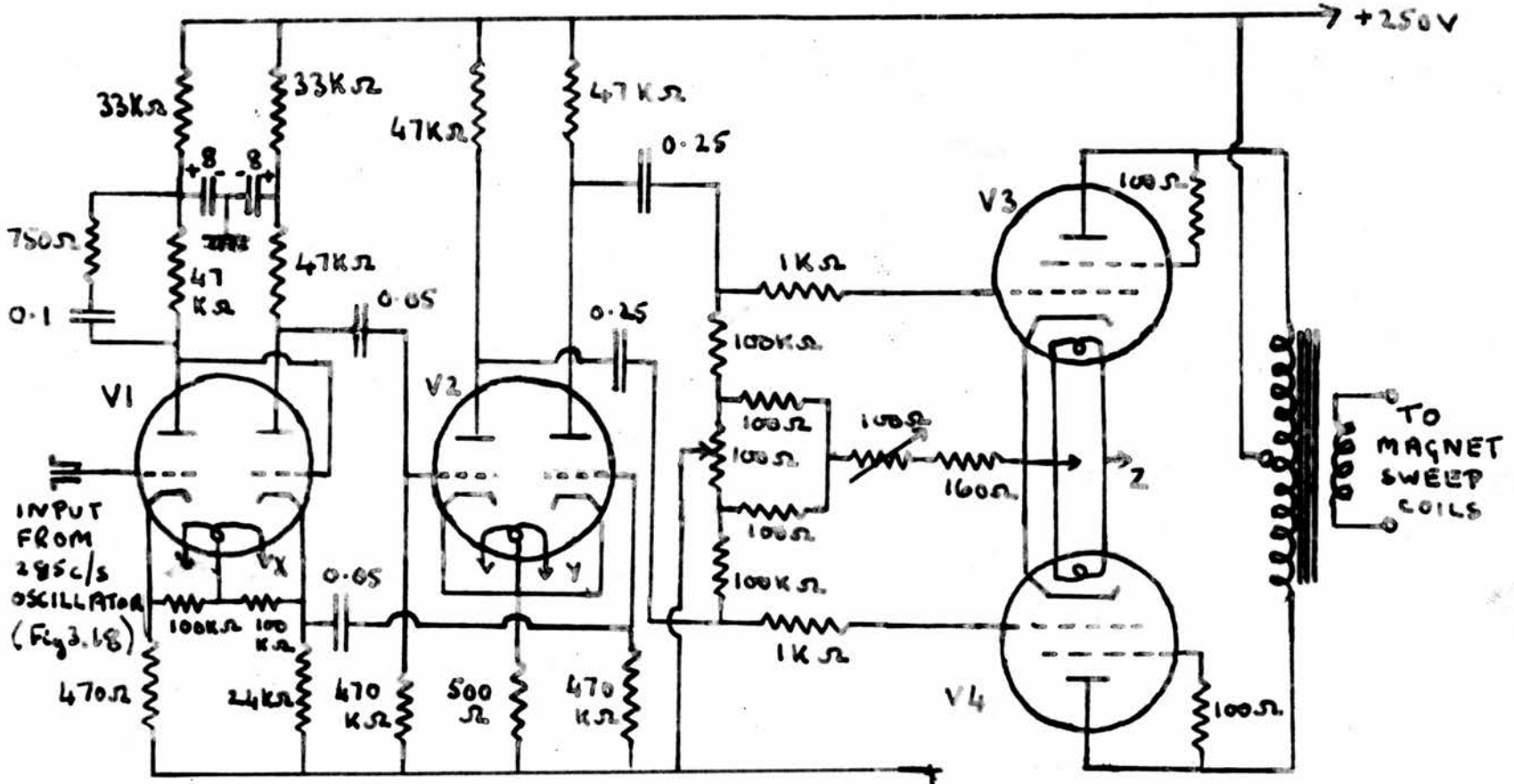

V1, V2 6SN7 All resistors ½W Heaters X, Y, Z. 6V AC.

V3, V4 KT66 All condenser values in μF.

Fig. 3.19. Power Amplifier for 285c/s Field Modulation

and the power amplifier unit were designed and constructed by Mr. I. M. Brown. Frequency variation of the first R-C oscillator stage is achieved by variation of the ganged 50 Kohm potentiometers of the R-C feedback network. This frequency variation is necessary since the oscillator and power amplifier are shared between two experimental stations working at slightly different detection frequencies. The thermistor in the oscillator stage helps to maintain constancy of oscillator amplitude. The buffer stages have two outputs. From the first anode a voltage is taken off to feed the phase-inverter stage which provides reference voltages of equal amplitude and opposite phase for the grids of the mixer valve, (Fig 3.21). From the cathode another smaller signal is fed to the grid of two further buffer stages, over which phase-variation of 180° of the output signal can be obtained using the gauged 500 Kohm potentiometers. Amplitude variation of the magnetic modulation is obtained using the 1 Mohm potentiometer across the output of the last buffer stage.

The power amplifier is constructed almost exactly to a design suggested by Williamson (W3, 4, 5). No feedback is necessary to improve the performance of the amplifier at 285 c/s. A cut-off filter for high frequencies is incorporated in the first stage of this amplifier (Fig. 3.19). The output is capable of producing 200V R.M.S. across the new sweep coils. The impedance of these

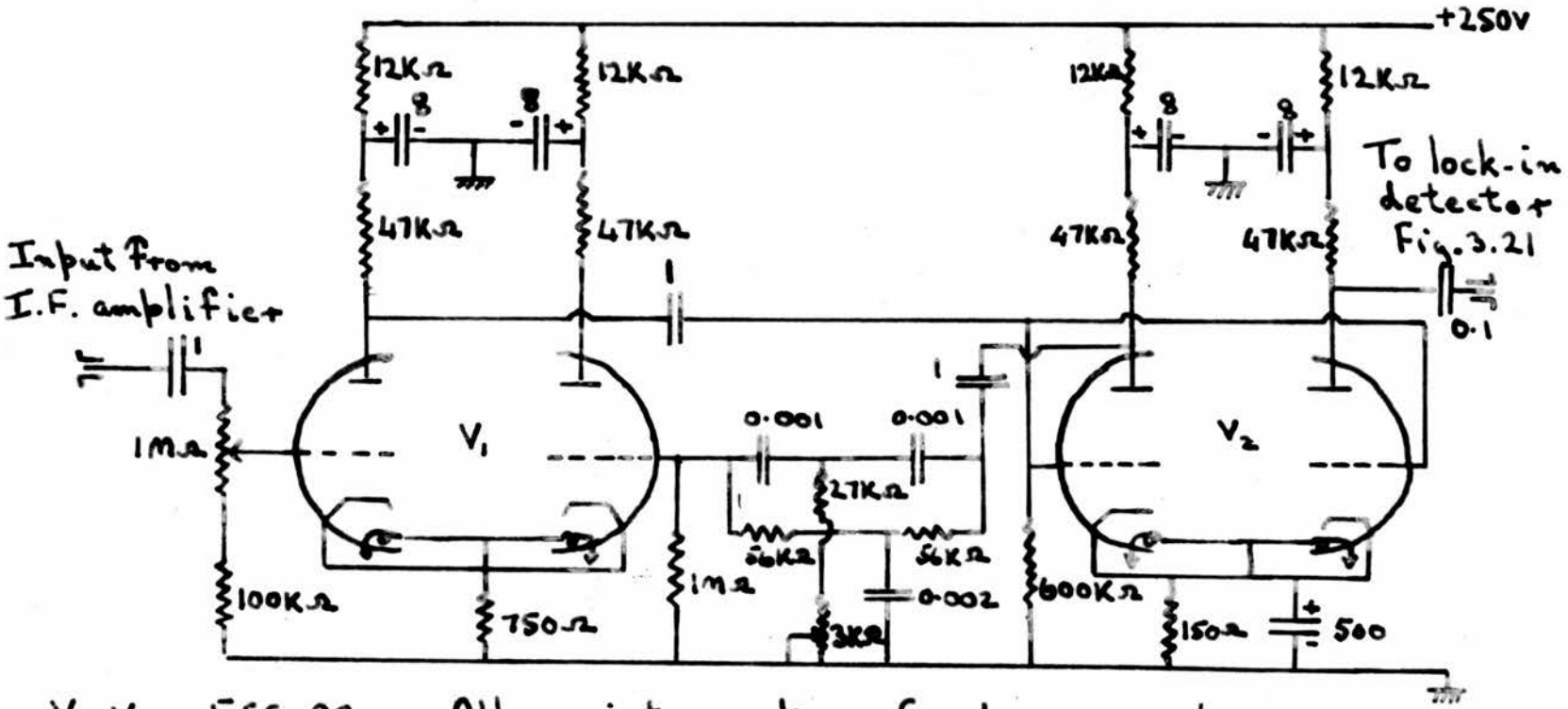

V_1, V_2 ECC 83 All resistors ½W. Condenser values in μF.
Heaters 6·3V A.C.

Fig. 3.20 285 c/s Amplifier ; 4 c/s Bandwidth ; Gain ~ 800.

coils in parallel is 1,800 ohm at 285 c/s, so that maximum power output of the amplifier is just over 20W. This corresponds to a peak-to-peak magnetic modulation of approximately 60 gauss, which is far more than enough for our purpose.

The detected output of the I.F. amplifier is fed to the input of the narrow band amplifier shown in Fig. 3.20. This is a simple two-stage triode amplifier employing twin-T feedback in such a way that the overall gain of the amplifier is in no way affected by the shunting effect of the twin-T. The amplifier voltage from the first stage is fed to the grids of two equivalent second stages. From one of these is taken the feedback signal, and the other feeds the amplified signal into the lock-in-detector circuit. The feedback is electron-coupled to the cathode circuit of the first stage, since direct coupling to the cathode would shunt the twin-T reducing its effective Q. With this arrangement the amplifier has a gain of 800 and a bandwidth of 4 c/s. Any alteration in the amplitude of the output of this amplifier is achieved by cutting down the input signal with the input potentiometer before the signal is amplified. In this way the high Q-factor produced by high gain is maintained. The signal entering the lock-in-detector is thus confined to components whose frequencies lie in the range 285 c/s $\pm$ 2.

The phase-sensitive detector and its associated circuits are shown in Fig. 3.21. The mixer circuit is of a type originally

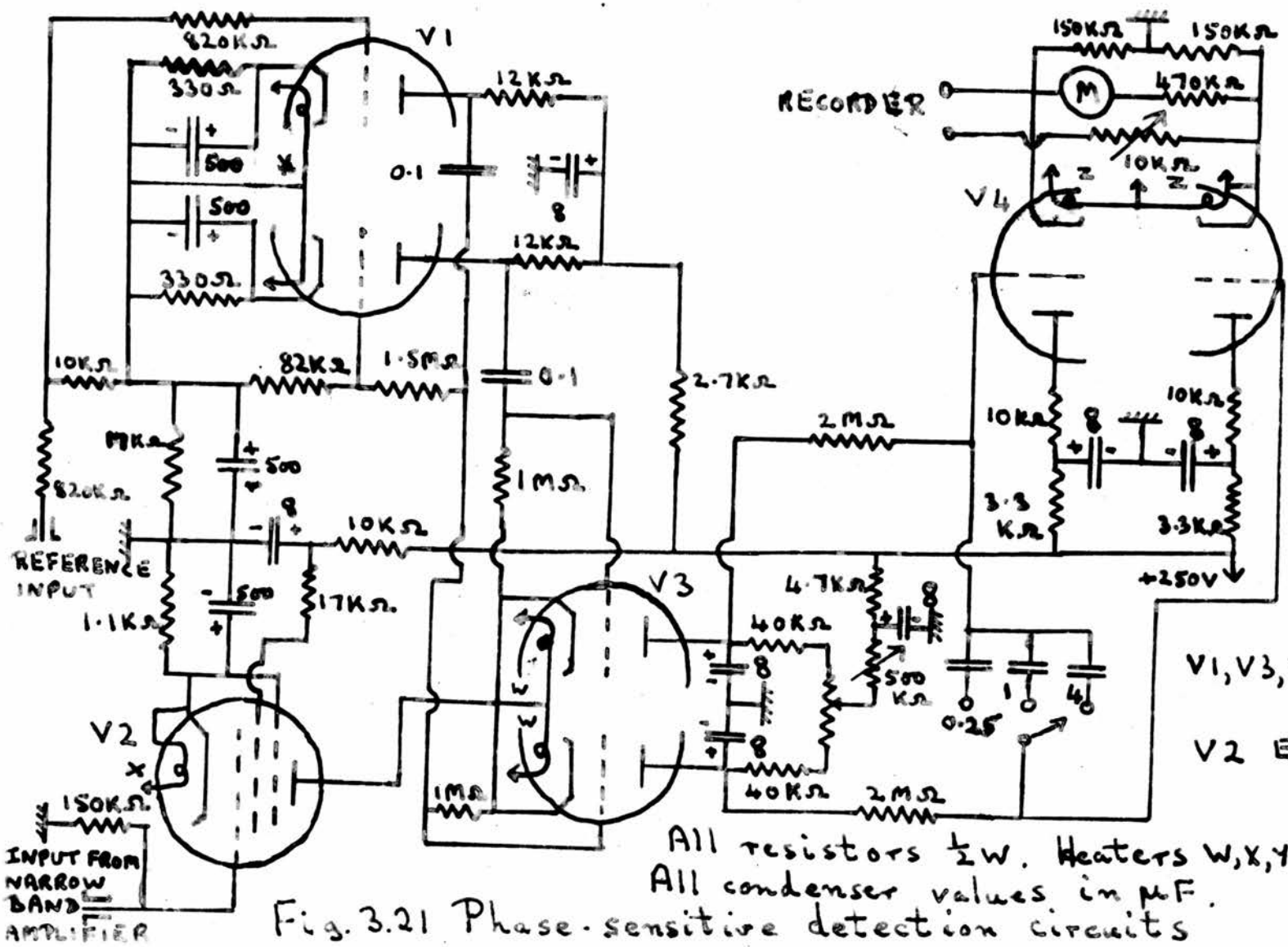

All resistors ½W. Heaters W,X,Y,Z 6·3V A.C
All condenser values in μF.

Fig. 3.21 Phase-sensitive detection circuits

suggested by Schuster (S1) which retains its balance despite changes in the characteristics of the two halves of the mixing valve, by virtue of the large anode resistance of the pentode tube in its cathode circuit. The signal from the narrow band amplifier is fed to the grid of this pentode and appears unamplified at the cathode of the mixing tube, whose grids are fed with reference voltages equal in magnitude - about 20V peak-to-peak - and opposite in phase. The best sensitivity of this detecting circuit is obtained when the phase of the incoming signal at the cathode of the detector valve is the same as that of one reference signal. As the D.C. field is swept slowly through an absorption the relative potential between the anodes of the detector valve changes. This change is passed via a variable R.C. filter, directly to the final D.C. amplifier stage, the pen-recorder being connected between the cathodes of this final stage and registering relative differences in cathode voltage. The time-constants which may be selected from the R.C. filter are 1, 2 and 4 seconds.

The pen-recorder used was an Evershed and Vignoles Murday recording ammeter, maximum deflection $\pm$ 0.5 mA. Variable chart speeds can be obtained for use with different line widths.

(3.i.) Scope Display

The various pictures obtained from the oscilloscope display points 1 to 6 (Fig. 3.2), may be switched in to the oscilloscope

screen. Typical examples are shown in Fig. 3.22.

(a) At point 1, with synchronised saw-tooth sweep on the signal klystron reflector, the reflected pattern from the cavity arm is displayed for the whole klystron mode. The matched cavity dip is shown, together with the smaller dip due to the abstraction of incident energy by the wavemeter. An estimate of the order of magnitude of the loaded Q of the cavity may be obtained from this curve, though this method is only accurate for a transmission cavity (D2). The width of the cavity dip is compared with the known total width of the klystron modes.

(b) At liquid helium temperatures the Q of the cavity is enhanced by virtue of the decreased losses in the cavity walls. The effect is shown here and should be compared with (a), where the cavity dip is much broader with respect to the wavemeter dip.

(c) Resonance lines of large samples may be observed at this crystal when a large amplitude 50 c/s magnetic modulation is applied to the sweep coils. The line shown is the main line of a specimen of neutron irradiated MgO. Smaller satellite lines are just visible to the right and left of the main lines.

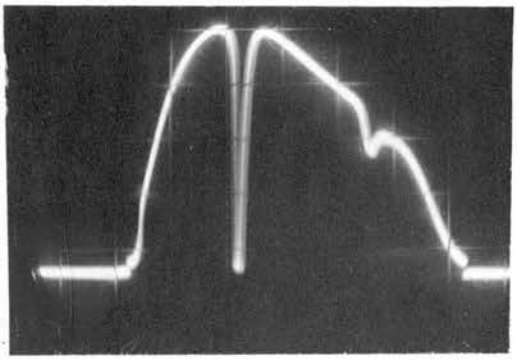

a) Signal klystron mode display showing matched cavity dip and the smaller wavemeter dip viewed at crystal A.

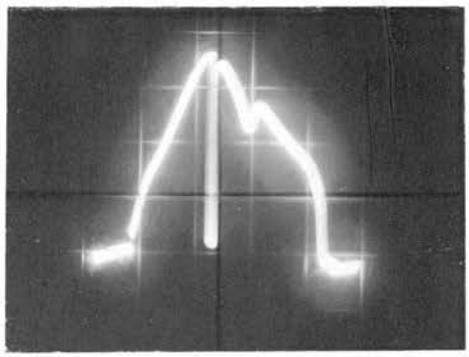

b) The same display as (a) with the cavity at 4.2°K, shows the increase in cavity Q as a narrowing of the cavity dip.

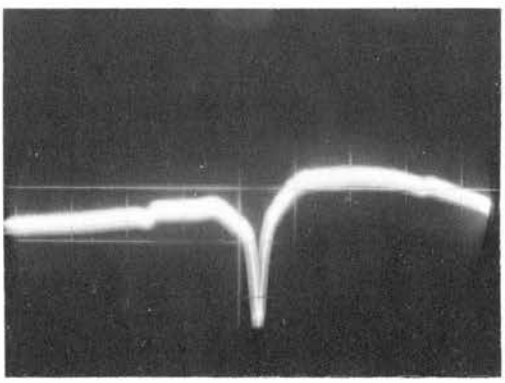

c) Straight detection at crystal A of a neutron-irradiated MgO specimen at 4.2°K. The main line and two satellites are shown.

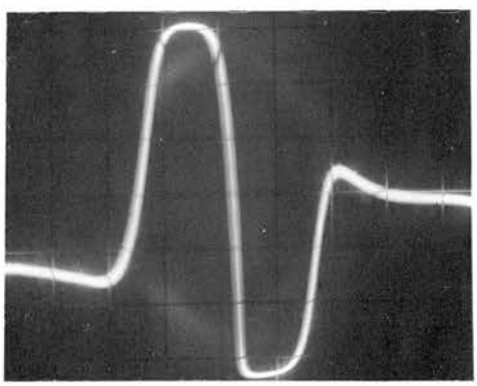

d) The signal klystron stabilisation curve. Peak-to-peak voltage is 70V.

Fig. 3.22. Oscilloscope Display Curves.

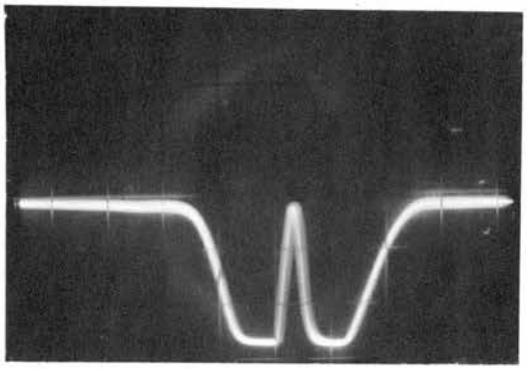

e) The I.F. amplifier response curve showing the cavity dip in the centre.

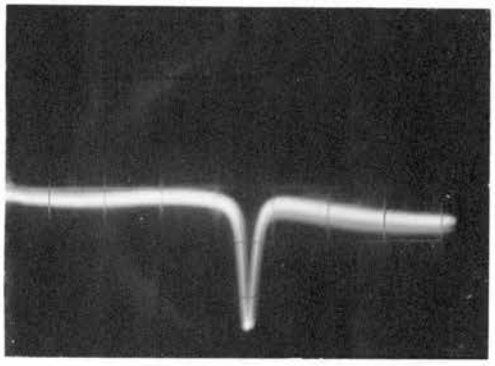

f) Video detection of a DPPH resonance from a sample containing 10^{17} spins.

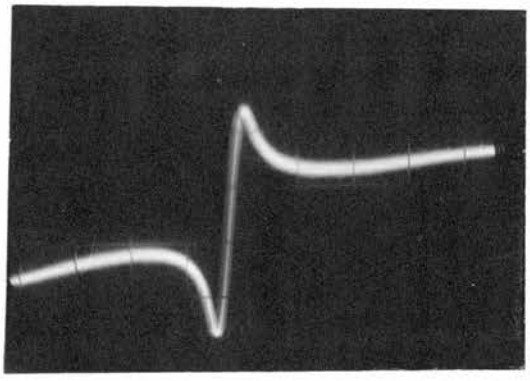

g) The effect of slight detuning of the cavity on the signal in (f) is shown.

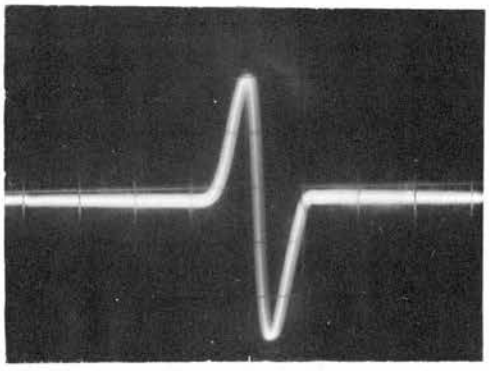

h) The AFC correction curve. Peak-to-peak voltage is 60V.

Fig. 3.22. Oscilloscope Display Curves.

(d) At 2 the output of the signal klystron control circuit is shown for all reflector voltages of the klystron mode, showing clearly the S-shaped correction curve of the cavity. The peak-to-peak value here is 70V.

(e) The I.F. amplifier response curve is shown at 3. The signal klystron is again swept. The cavity dip is in the centre of the response curve, showing that I.F. output is a minimum on the cavity resonance. The amplifier output is first passed through a 5 Kc/s low-pass R.C. filter.

(f) The video display of a DPPH resonance absorption signal is shown at 3.

(g) The video display of a DPPH resonance absorption when the cavity is slightly detuned. An admixture of dispersion and absorption is obtained.

(h) The A.F.C. correction curve is shown at 4. Peak-to-peak value is 60V. The signal klystron was swept for this display.

At 5 the input signal at the cathode of the phase-detector valve is shown, an almost pure 285 c/s sine wave and resonances are detected by changes in the amplitude of this signal. The phase of the magnetic modulation is adjusted until this signal is in phase with one of the reference voltages shown at 6. 5 and 6 are viewed on a small double-beam oscilloscope, the signals being synchronised together.

(3.j.) The Alignment of the Spectrometer

All the electronic units are switched on, starting with the klystron repeller and heater battery supplies, with the signal klystron stabilisation and AFC switches in position 2, the sweep position. A saw-tooth sweep is applied to the reflector of the signal klystron and a thorough check is made to see that all parts of the spectrometer are functioning properly, by means of oscilloscope display and the incorporated voltmeters and ammeters. The 285 c/s oscillator is then frequency aligned to the narrow band amplifier.

The signal klystron is then locked to the resonant frequency of the cavity as explained in (3.b.(v)). The AFC is brought into operation as explained in (3.b.(vii)).

The spectrometer is now ready to record spectra and the gains of the I.F. amplifier and narrow-band 285 c/s amplifier may be adjusted according to the intensity of signal expected.

CHAPTER 4

The Sensitivity of the Apparatus and Some Irradiation Experiments

(4.a.) Sensitivity

The sensitivity of the apparatus at room temperature has been judged using samples of DPPH in small cylindrical perspex holders, with central sample holes of diameters 1 and 2 mm., whose caps press on in a tight fit. The smallest sample that could be weighed contained 10^{17} free spins. Two attempts to make smaller samples have been made. In the first of these DPPH was mixed in an electric mixer with a known weight of dry chalk and the mixture then weighed into similar sample holders. No absorption signals were obtained from any of these samples. In the second attempt successive dilutions, by factors of 5, of DPPH in benzene were made. At each dilution a sample-holder cavity was filled with the solution using a medical syringe. When the benzene had evaporated the caps of the sample-holders were pressed in. Knowing the approximate volume of the sample-holder cavity and the dilution of the solution estimates of the number of radicals in each sample were made. The estimated samples ranged from 10^{17} down to 2×10^{14} spins, and all these samples yielded signals of the correct order of magnitude at room temperature in the most sensitive spectrometer in the laboratory.

Sensitivity considerations in 3-cm. paramagnetic resonance

spectrometers are discussed in F9. Assuming that our cavity is correctly matched to tee 1 the sensitivity of our spectrometer is limited by the following:-

(i) The Q factor of the cavity.

(ii) The signal klystron power.

(iii) Mixer crystal noise and I.F. amplifier noise.

(iv) Microphonics.

We discuss these effects as related to the spectrometer and point out factors which could improve the sensitivity.

(i) The loaded Q of the cavity has been estimated to be about 3,000. This could be improved by constructing the cavity in one piece. A rectangular H_{012} cavity used in another spectrometer in the laboratory has given a higher Q.

(ii) With the signal klystron power available we have been unable to saturate any of the resonance lines examined. Increase in signal klystron power could yield enhanced sensitivity until saturation is reached.

(iii) Mixer crystal noise is negligible at 45 Mc/s but could be completely eliminated by the use of a balanced mixer arrangement at the mixer tee 2. This can be easily effected by the use of the two crystal mounts in the side arms of the mixer tee.

Unfortunately an I.F. amplifier with a suitable input stage could not be obtained. This crystal noise is not, however, the limiting factor in the sensitivity of our spectrometer.

Noise arising within the I.F. amplifier itself has not been troublesome, since most 50 c/s noise was removed by heating the valves with D.C. A low-pass R.C. filter is placed in the output of the amplifier to remove R.F. noise components before oscilloscope presentation or before passing the signal to the phase-sensitive detection circuits.

(iv) Microphonics and 50 c/s pick-up have been the most troublesome noise sources in our spectrometer. 50 c/s pick-up has largely been eliminated as experience of operating the spectrometer was gained but microphonics from the cavity are the limiting factor on the sensitivity using phase-sensitive detection. The microphonics are believed to be due mainly to the looseness of the screw coupling between the two halves of the cavity. They arise from the interaction of the magnetic modulation with eddy currents in the cavity walls. At high spectrometer gains this results in jitter on the pen-

a) Phase-sensitive detection of the absorption signal from a DPPH specimen of 10^{16} spins.

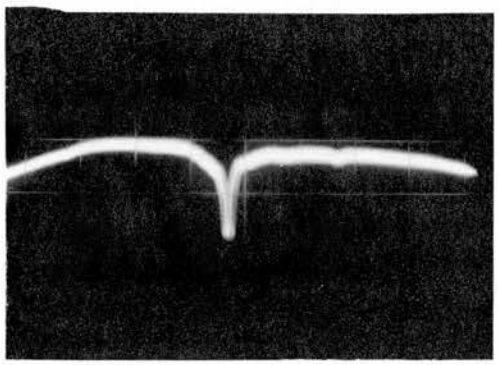

b) Room temperature video absorption signal from the same MgO specimen as in Fig. 3.22(c).

Fig. 4.1.

recorder, which lessens as the current through the sweep coils is lowered and vanishes altogether when this current is switched off. The advantage of a one-piece cavity free from such vibrations is obvious.

At room temperature using video detection a signal-to-noise ratio of 1:1 is obtained with a DPPH specimen containing 10^{16} spins. A pen-recorder trace obtained from the same sample is shown in Fig. 4.1(a). Here the signal-to-noise ratio is at least 20:1, and the I.F. and narrow-band gains cannot be made larger without excessive pen-recorder jitter.

For a comparison of the video-sensitivities at room temperature and 4.2°K observations were made on a neutron-irradiated MgO sample. The room-temperature signal obtained from the main line has a signal-to-noise ratio of about 6:1, Fig. 4.1(b). The same sample at 4.2°K gave a signal to noise ratio of about 500:1 showing that the sensitivity is increased about 80 times. This is more than the factor 56 due to change in population difference calculated in Chapter 2. The extra difference is due to the increased Q of the cavity at low temperature. It should be realised that these figures are only approximate since experimental conditions cannot always be repeated identically. We make conservative estimates of the sensitivity of the spectrometer as indicated below. The sensitivity

is given in terms of the number of free spins in DPPH samples with 2.7 gauss line width.

Temperature	Video sensitivity	Pen-recorder sensitivity
Room	10^{16} spins	5×10^{14} spins
$4.2^{\circ}K$	2×10^{14} spins	10^{13} spins

It should be borne in mind that this table gives the minimum detectable signal. For good recording of a complex spectrum the number of spins should be 10 to 100 times greater.

Another indication of increased sensitivity at helium temperatures is shown in Fig. 3.22(c). This is the straight-detected signal from A of the neutron irradiated specimens of MgO at $4.2^{\circ}K$. No signal can be detected here from the same specimen at room temperature. The ratio of the sensitivity indicated for straight detection with this arrangement, to that with video display after superheterodyne detection is 1:200 which gives an indication of the superiority of the superheterodyne system.

(4.b.) Irradiation Experiments

Four compounds have been irradiated at both liquid air and liquid helium temperatures for periods ranging from five to twelve hours. Some of these experiments were performed with the quartz light-pipe and others with the later optical arrangement. Some of the first of these experiments were repeated using the later arrangement. In none of the experiments were free radicals detected.

(i) Stilbene

Stilbene, s-diphenylethylene, is a white crystalline solid which exists normally in the trans configuration. At room temperature U.V. irradiation converts it to the liquid cis form.

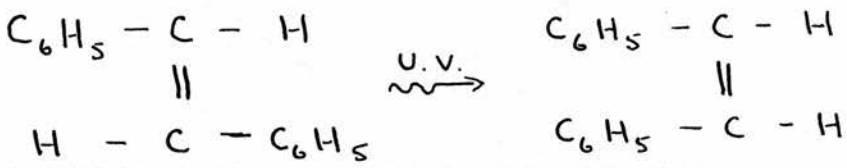

Photoionisation or breakage of bonds might be expected to yield a concentration of free radicals at low temperatures.

The stilbene crystals were compressed into a small pill prior to illumination and the pill was stuck to the bottom of the cavity with a little nail-varnish.

(ii) p-phenylenediamine and tetra-methyl-p-phenylenediamine

The products of the photochemical dissociation of these molecules have been investigated by U.V. absorption spectra (Ll,2,3,4,5) using the trapping technique with E.P.A. glass. Bijl and Rose-Innes (Rl) obtained paramagnetic resonance absorption signals from these compounds using low and room temperature trapping techniques. The crystals were first washed in benzene to remove the coloured oxidation layer which inevitably forms on them and which might absorb the U.V. light before penetration to the clear crystal inside. Photoionisation radicals are the most likely yield.

(iii) Hexamethylbenzene

The interpretation of the spectra of free radicals created by dissociation should be of interest since the molecule is planar. The most likely radical is the positive ion which is planar also.

(4.c.) Some Suggestions for Future Use and Development

The spectrometer is at present suitable for the recording of paramagnetic resonance spectra of stable solid free radicals at temperatures down to $1^{\circ}K$. These could include solids with permanent X- or γ -ray damage containing a sufficient number of spins to give good signals. The number necessary will vary with the line width but would be of order 10^{17}.

For successful completion of the experiments already attempted a new cryostat would probably be required in which the U.V. light could be focussed on the sample from a distance of only a few inches. This would require a Dewar vessel with a quartz window and a cavity of rectangular shape with quartz rod tuning and a window in the narrow side to admit the light. Careful focussing of the light would be necessary.

We have already seen that such a cavity would reduce microphonics considerably. The resulting increase in spectrometer sensitivity combined with the increased radical yield due to the better U.V. optical system could perhaps lead to successful results of the type hoped for.

REFERENCES

A1 Anderson, P.W. and Weiss P.R.; Rev. Mod. Phys., 25, (1953), 269

B1 Bijl, D. and Rose-Innes, A.C.; Nature, 175, (1955), 82.

B2 Bloch, F.; Phys. Rev., 70, (1946), 460.

B3 Bloembergen, N., Purcell, E.M. and Pound, R.V.; ibid, 73, (1948), 671.

B4 Bleaney, B. and Stevens, K.W.H.; Rep. Prog. Phys., 16, (1953), 108.

B5 Bowers, K.D. and Owen, J.; ibid, 18, (1955), 304.

D1 Dirac, P.A.M.; Principles of Quantum Mechanics, O.U.P.

D2 Ditchfield, C.R.; R.R.E. Technical Note, No. 639, (1958).

F1 Farmer, F.T.; Nature, 150, (1942), 521.

F2 Fowler, J.F. and Farmer F.T.; ibid, 171, (1953), 1020.

F3 " " " " " " ; ibid, 173, (1954), 317.

F4 " " " " " " ; ibid, 174, (1954), 136.

F5 " " " " " " ; ibid, 174, (1954), 800.

F6 " " " " " " ; ibid, 175, (1955), 516.

F7 " " " " " " ; ibid, 175, (1955), 590.

F8 " " " " " " ; ibid, 175, (1955), 648.

F9 Feher, G.; Bell Syst. Tech. J., 36, (1957), 449.

H1 Hutchison, C.A., Pastor, R.C. and Kowalsky, A.G.; J. Chem. Phys., 20, (1952), 534.

H2 Huxley, L.G.H.; "Waveguides", C.U.P., (1947), 82.

I1 Ingram, D.J.E.; "Free Radicals as studied by Electron Spin Resonance", Butterworth, (1958).

K1 Kommandeur, J. and Schneider, W.G.; J. Chem. Phys., 28, (1958), 500.

K2 Kivelson, D.; ibid, 27, (1957), 1087.

L1 Lewis, G. N. and Lipkin, D.; J. Am. Chem. Soc., 64, (1942), 2801.

L2 Lewis, G. N. and Bigeleisen, J.; ibid, 65, (1943), 520.

L3 " " " " " " ; ibid, 65, (1943), 2419.

L4 Lewis, G. N. and Calvin, M.; Chem. Rev., 25, (1939), 273.

L5 Lewis, G. N. and Bigeleisen, J.; J. Am. Chem. Soc., 65, (1943), 2424.

L6 Lowe, G.C.; Elect. Eng., 31, (1959), 138.

M1 Meyer, R. A., Bouquet, F. L. and Alger, R. S.; J. Appl. Phys., 27, (1956), 1012.

M2 Montgomery, C. G.; "Technique of Microwave Measurements", Vol. 11, M.I.T. Radiation Laboratory Series, McGraw-Hill, 527.

P1 Pauling, L. and Sherman, J.; J. Chem. Phys., 1, (1933), 606.

P2 Pryce, M. H. L. and Stevens, K. W. H., Proc. Phys. Soc., A63, (1950), 36.

P3 Pound, R. V.; "Microwave Mixers", Vol. 16, M.I.T. Radiation Laboratory Series, McGraw-Hill, 263.

R1 Rose-Innes, A. C.; Ph.D. Thesis, Oxford, (1954).

R2 Ragan, G. L.; "Microwave Transmission Circuits", Vol. 10, M.I.T. Radiation Laboratory Series, McGraw-Hill, Ch. 8.

S1 Schuster, N. A.; Rev. Sci. Instr., 22, (1951), 254.

T1 Torrey, H. C. and Whitmer, C. A.; "Crystal Rectifiers", Vol. 15, M.I.T. Radiation Laboratory Series, McGraw-Hill, 353.

V1 Van Vleck, J. H.; Phys. Rev., 74, (1948), 327.

W1 Whiffen, D. H. and Atherton, N. M.; Mol. Phys., 3, (1960), 1.

W2 Whiffen, D. H., and Ghosh, D. K.; ibid, 2, (1959), 285.

W3 Williamson, D. T. N.; Wireless World, 53, (1947), 118.

W4 " " " " ; ibid, 53, (1947), 161.

W5 " " " " ; ibid, 55, (1949), 282.

APPENDIX

Microwave Equipment Used in the Spectrometer

Klystrons	English Electric, Type K302.
Sliding Stub Tuner	Microwave Instruments, Type 32/1400.
Wavemeter	Microwave Instruments, Type 32/2000. Serial No. 638F.
Flexible Waveguide Coupling	"Flexiguide", W. H. Sanders, (Electronics), Limited.
Directional Coupler	Microwave Instruments, Type 32/1700.
Attenuators	Microwave Instruments, Type 32/670.
Ferrite Isolators	Microwave Instruments, Type 32/4010.
Waveguide Bends	Microwave Instruments, Type 32/2950.
Magic Tee	Phi l ips, Type PP 4050X.
Waveguide	"Azdar", Waveguide No. 16, Brass.
Couplers	"Contar", Type 54/EV/5164.

ACKNOWLEDGEMENTS

I gratefully acknowledge the help of the following:-

Prof. J. F. Allen, F.R.S.:	for his interest and the facilities of the University of St. Andrews Physics Research Laboratory.
Dr. D. Bijl:	for his supervision and encouragement.
Dr. C. K. Campbell and Messrs. R. A. Beveridge, I. McL. Brown and I. M. Firth:	much of the work of design and testing was shared with these co-workers in the microwave section of the Laboratory.
Mr. J. Gerrard:	for his assistance with the drawings and photographs, and in the ordering of equipment.
Mr. R. H. Mitchell:	for his never-complaining efforts to maintain a frequent supply of liquid helium.
Mr. H. Cairns:	for assistance with electrical components.
Messrs. J. MacNab, T. Marshall, M. Bird, G. Dunsire, F. Akerboom, and E. Pirie.	for the construction of many parts of the apparatus and their willingness to help an ignorant amateur mechanical engineer.
Miss M. E. Noble:	for a quick and efficient piece of typing.
Imperial Chemical Industries, Limited, The Department of Scientific and Industrial Research and The University of St. Andrews:	for the award of maintenance grants.